9-28-2021

Delivery Optimization and Evaluation of Biomechanics of an Injectable Nucleus Pulposus Replacement Device

Zachary Rustin Brown
Rowan University

DELIVERY OPTIMIZATION AND EVALUATION OF BIOMECHANICS OF AN INJECTABLE NUCLEUS PULPOSUS REPLACEMENT DEVICE

by

Zachary R. Brown

A Thesis

Submitted to the
Department of Biomedical Engineering
College of Engineering
In partial fulfillment of the requirement
For the degree of
Master of Science in Biomedical Engineering
at
Rowan University
August 4, 2021

Thesis Advisor: Erik Brewer, Ph.D.

Committee Members:
Anthony Lowman, Ph.D.
Gary Thompson, Ph.D

Abstract

Zachary R. Brown
DELIVERY OPTIMIZATION AND EVALUATION OF BIOMECHANICS OF AN INJECTABLE NUCLEUS PULPOSUS REPLACEMENTDEVICE
2020-2021
Erik Brewer, Ph.D.
Master of Science in Biomedical Engineering

Lower back pain effects up to 80% of people at some point in their life, a majority of cases being the result of degenerative disc disease. Treatment options for degenerative disc disease are limited, jumping from physical therapy to major spinal fusion and total disc replacement surgery with little to no approaches in between. Furthermore, surgical treatments have not shown to be more effective than conservative treatments and reducing pain and disability over the long term. Hydrogels have shown promise as a potential nucleus pulposus replacement device. In order to successful act as a minimally invasive nucleus pulposus replacement device, the hydrogel must demonstrate an ability to be easily injectable, cure within the body, and restore mechanics once in place.

One potential formulation to complete this task is HYDRAFIL™. HYDRAFIL™ is a PVA/PEG based hydrogel designed as a nucleus pulposus replacement device. HYDRAFIL™ demonstrates thermosetting properties that can be controlled through the use of thermal cycling and holding the material at elevated temperatures until injection. Through various mechanical tests and thermal analyses, HYDRAFIL™ demonstrated the ability to cure within the disc and act as a solid implant. After curing HYDRAFIL™ exhibits substantial mechanical strength and desired hydration properties.

Table of Contents

Table of Contents (Continued)

Table of Contents (Continued)

List of Figures

List of Figures (Continued)

Figure Page

List of Tables

Chapter 1

Introduction

1.1. Gap in Care

Low back pain is the most prevalent musculoskeletal problem globally and the leading contributor to years lived with a disability [1]. Up to 80% of adults experience back pain at some point in their lives [2]. One of the leading causes of low back pain is degeneration of the lumbar spinal discs [3]. By age 40, about 40% of people experience some extent of disc degeneration. This rate increases to 80% by age 80 [4]. This financial burden of degenerative disc disease in the US is estimated to be between $560-$635 billion annually [5].

Currently, options are limited between conservative and aggressive treatments. Patients typically move from physical therapy and pain medications to highly invasive surgeries such as spinal fusions with no options in between [6]. These options that do exist also have limited effectiveness. Reoperation rates of fusion surgeries are around 19% after 4 years [7]. There is no significant difference in the outcomes of patients who choose physical therapy over fusion [8].

Some of potential treatments to bridge this gap include cell therapies, annulus fibrosus repair technologies, and nucleus pulposus replacements [9][10]. Cell therapies show great theoretical promise but have yet to be used in a human clinical trial. Annulus fibrosus repair technologies are currently limited in their ability to integrate with native tissue and aide in biomechanics [11].

Nucleus pulposus replacement devices aim to restore the mechanics of the

disc to alleviate pain, instead of just augmenting the diseased tissue. Nucleus Pulposus replacement devices may be created using curable polymers and hydrogels that are cured either inside the body, or outside the body and then implanted [12]. Technologies formed outside the body are prone to migration in the disc space [13]. Injectable devices can minimize the risk of migration or expulsion; however they are subject to the flow conditions of the material. Once in the body they must also be mechanically strong enough to support loads in the spine and restore biomechanics [9].

Hydrogels traditionally have not been consider suitable for load bearing applications like disc replacements, but studies have shown exceptional mechanical strength in confined conditions, such as an annulus fibrosus [14]. *In situ* curing hydrogels can both satisfy this mechanical need and fill in the gap in coverage for degenerative disc disease [9].

1.2. HYDRAFIL™

HYDRAFIL™, an injectable hydrogel designed to mimic the biomechanical properties of the spine and preserve motion, was evaluated in this work to determine the optimal delivery conditions, characterize the curing properties, and determine the effects on biomechanics [15]. Tests were designed to determine conditions that should be met for successful implantation of the device and the effects the device has on the mechanics of the spinal disc.

For delivery of HYDRAFIL™, properties such as gelation and crystallization must be understood and controllable to ensure flow of the hydrogel. Both crystallization and gelation increase the modulus of the gel and its solid properties, increasing shear forces

during injection or precenting flow completely. Reversibility of crystallization and gelation is essential to successful implantation of the device. Thermal cycling has been successfully used to reverse these in similar gels in previous studies [16][17]. Autoclaves are used to achieve sufficiently high enough temperatures to restore flow of HYDRAFIL™. Therefore, differential scanning calorimetry (DSC) was used in this work to determine conditions that promote crystallinity and evaluate the effectiveness of an autoclave cycle at reversing it. Rheology was used to determine under what thermal conditions that gelation occurs and what temperature is required to hold the gel in a flowable state.

Once delivered to the spinal disc, HYDRAFIL™ must be able to gel under body conditions (37°C) [16]. After the gel has cured it must not migrate outside the annulus once loaded [11]. Rheological tests were used to determine how quickly HYDRAFIL™ gels under body conditions. Mechanically loading surrogate annuli can mimic forces experienced by the gel during an injection. To better understand the expulsion mechanisms and how they relate to gelation, tests were developed to determine the amount of time it will take for the gel to resist expulsion after injection. Gels should also be able to recover lost hydration from storage and equilibrate with the disc tissue under similar swelling conditions as the body. Hydration recovery tests were developed to examines the gel's ability to regain lost water during storage.

After the gel has cured, it must be able to function as a nucleus pulposus. In order to accomplish that, the gel must demonstrate an ability to recover water lost due to mechanical cycling, demonstrate high mechanical strength under confined conditions and increase stiffness once implanted, and integrate with existing disc tissue [14]. A

mechanical testing machine was used to simulate typical cyclic forces experienced through the day, and then unloaded during a “sleep” cycle in an osmotic swelling solution to measure the gel’s ability to recover hydration. Compression tests were used to evaluate the gels strength under confinement and measure impact the gel has on stiffness in cadaveric spinal discs. To quantify biointegration, the force to extract the implant from a cadaveric annulus was measured by pulling on the implant axially from the annulus.

Chapter 2

Background

2.1. Anatomy

2.1.1. Vertebral Column

The vertebral column is made up of vertebrae and spinal discs. It contains three mobile segments: cervical, thoracic, and lumbar. There are 7 cervical, 12 thoracic, and 5 lumbar vertebrae. The lumbar section is attached to two immobile spinal segments, the sacrum and coccygeal, which are made of fused vertebral bodies [18]. Due to a primarily bipedal movement, human spines have developed unique anatomical changes. In utero the spine is in complete flexion, typical to other mammals. As a child learns to hold its head up, sit upright, and walk it will begin to develop curves in the vertebral column. A typical adult has 5 curves in their spine from a sagittal view, while an infant only has a bend in the sacrum from birth [19]. These curves develop to allow muscles and ligaments absorbs some loads experienced by the spine. Without these, all loads would be completely transmitted through the spinal discs. As loads increase going down the spine, vertebrae and spinal discs tend to get larger to better distribute the load. Quadrupeds tend to have uniformly sized vertebral bodies [20].

Functions of the vertebral column include trunk control, transfer of loads, head movement and stabilization, and protection of the spinal cord and nerve roots. The spine allows for three degrees of freedom. Flexion and extension, both laterally and anteriorly, and rotation about the spine's axis. The spine is anchored by the pelvis. Abdominal and back flexion bridge these areas and control motion of the spine. Dynamic loads in the spine are distributed through spinal discs, muscle/ ligaments, and nonstructural bends in

the spine [21][22]. The vertebrae are the primary protection for the spinal cord and nerve roots. Spinal processes protrude from the vertebral bodies providing protection for nerve roots and create the neural arch on the posterior side to protect the spinal cord [23]. The cord runs through the posterior side of the vertebrae, below the lamina. Roots extend from the spinal cord laterally between the vertebrae. Due to the close proximity with these tissues, pathologies effecting the spine often leads to damage and irritation of the spinal cord and nerve roots [21].

As the spine experiences loads and activity, forces experienced by the spinal discs are balanced by the swelling pressure of the tissue to create a hydrostatic pressure within the disc. The hydrostatic pressure is a reactionary force to the loads that the spine experiences. It aids in the tissue's ability to absorb compressive forces transmitted by the vertebrae. The tissue in this situation acts very similar to hydraulic shocks or dampeners, where it is a fluid under pressure that is providing smooth resistance to loads [24].

2.1.2. Spinal Disc

The intervertebral disc is comprised of two main parts, the annulus fibrosus and the nucleus pulposus. It is the largest avascular structure in the body [25]. Vertebral end plates contain the disc on either side and are the primary median for nutrient diffusion into the disc tissue. The annulus fibrosus is primarily made up of collagen I and elastin. These proteins are formed into roughly 10 to 20 lamella layers. Collagen Fibers in the lamella layers are oriented 65 to 70 degrees from the longitudinal axis of the body [26]. These layers are not typically separate circular pieces, but rather fused together at one point to the adjacent layer. The inner collagen fibers of the lamella come in direct contact with either end plate. The nucleus pulposus has an extracellular matrix made out of

glycosaminoglycan proteoglycans and collagen type II bound to water molecules. Approximately 80% of the nucleus pulposus by weight is water. This tissue is extremely viscoelastic and is often compared to a liquid [26].

Proteoglycans are attributed to the nucleus pulposus's ability to retain water and make up roughly 65% of the nucleus pulposus's dry weight. Proteoglycan and collagen synthesis for the nucleus pulposus is performed by chondrocytes [26]. Chondrocytes are mostly found in the endplates of the vertebrae. Since the nucleus pulposus tissue is avascular, it relies on chondrocytes to take nutrients from the bone marrow of the vertebrae, which comes in direct contact with the vertebral end plates. The cell viability of the chondrocytes diminishes with age, leading to a diminished synthesis rate of proteoglycans [26]. The proteoglycans in the nucleus pulposus are highly negatively charged, which is countered by positively charged interstitial fluid outside the nucleus pulposus. This charge difference creates an osmotic swelling pressure inside the nucleus pulposus, which is then contained by the annulus fibrosus and the vertebral end plates. The swelling pressure is a constant static force experienced by the tissue at all times and is not dependent on the dynamic loading experienced during walking or other physical activity. This creates constant tensile stresses inside the tissue that maintain its shape and structure [27].

Chondrocyte viability typically peaks around age 10. After this, cell viability constantly decreases leading to an increase in degeneration and dehydration of the disc. As a result, water content of the nucleus pulposus averages 85.3% in patients aged 14 and decreases to an average of 76.7% at age 91. This also causes a drop in swelling pressure, which is observed to be 0.19 MPa at age 37 and 0.05 MPa at age 91 [27].

2.1.3. Vertebral Endplates

Endplates are located at the top and bottom of each vertebra and interface with the spinal disc. They absorb and transmit significant forces through the spine and to the discs and are typically around 1 mm thick [25]. It is made up of a bilayer composed of bone and cartilage. As age increases, the cartilage layer thins as bone becomes more prominent. By adulthood, the subchondral bone plate has formed and is fully fused to the vertebral body [28].

The endplates are responsible for all nutrient transport into the disc. Oxygen, glucose, and waste movement must be done via diffusion through the endplate. Endplates make use of bone marrow channels and blood vessels in the vertebral body. These are more densely located near the center of the endplate where thickness of the endplate is lower allowing for increased permeability [28]. During development, blood vessels penetrate the endplate walls to provide nutrition to the disc, but then disappear as the body finishes growth [25].

2.2. Spine Mechanics

The spine is responsible for trunk control of the body and is the only structure that transmits force to the lower extremities. All loads being supported by the upper body must make use of the spine for strength and stability. Spine mechanics can be divided into two categories, active and passive [29]. Each vertebra is its own motion segment, allowing for flexion/ extension in both the frontal and sagittal plane, and rotation in the transverse plane. The focal points of these motions are not necessarily about the center of the spinal segment. This may change from vertebra to vertebra and is dependent on the direction of motion [30]. Each vertebral body in the motion segment of the spine is

capable of moving independently of the adjacent vertebrae. This leads to unique forces being distributed throughout the spine and allow for compressive, tensile, and shear forces to experienced simultaneously [31].

The spine is controlled by both intersegmental and multi-segmental muscles. Intersegmental muscles are believed to primarily provide stabilization to the spine (passive), while multi-segmental muscles primarily dictate motion of the spine (active) [29]. The largest of the multi-segmental muscles are the erector spinae. This group of muscles runs longitudinally along the spine. When acting bilaterally, the muscles are able to straighten the back, creating extension of the back and head. When acting unilaterally, these muscles create flexion in the lateral directions. The spinal thoracis is located between vertebrae T11 and L2 and is responsible for flexion of the thoracic section of the spine. The multifidus group of muscles fills in the spinal processes on either side and is primarily involved with lumbar extension, although this group is secondarily involved with both flexion and extension. These muscles span from L5 to C2, but are primarily developed in the lumbar section [32].

Passive muscles include short intersegmental muscles that connect the spinal processes of adjacent vertebrae. They are connected to both the medial branches and the dorsal rami. Their primary purpose is believed to be stabilization of the spine, although their location and size make this muscle group difficult to study [32]. Computer models have shown a drastic drop in stabilization of the spine without these muscles, suggesting that they do play a critical role in stabilization [29]. The Iliac muscle group also plays a role in stabilization. These muscles connect the lumbar section of the spine to the hip and

femur. While involved with hip abduction, it also provides stabilization to the upper half of the body [32].

When loads are applied to the spine, forces are primarily transmitted through the spinal discs. About 80% of the force experienced by the spine is experienced by the disc, while the other 20% is taken up by intersegmental muscles [33]. Loads are primarily taken by the nucleus pulposus, which generates a hydrostatic pressure within the tissue. This hydrostatic pressure distributes force across the vertebral endplates and the annulus fibrosus [34]. This mechanism slows the rate that force is applied to the anatomy and acts as shock absorption within the spine [35]. Asymmetric loading of the spine can lead to migration of the nucleus pulposus, where the NP will move opposite of where force is being applied. For example, flexion of the spine creates high compressive forces in the anterior side of the disc and will cause to NP to migrate towards the posterior side. This movement is predictable in healthy discs, but can become variable with increased degeneration [36]. Migration of the NP under loads can contribute to the herniation of the disc. Disc that are degenerated or have large transdiscal tears can create a pathway for herniation during the NP migration.

2.3. Degenerative Disc Disease

Nontraumatic degenerative disc disease is attributed to a loss of water in the disc. This leads to a decrease in disc height and ultimately a loss of mechanical properties. The primary cause of this dehydration is the nucleus pulposus losing its ability to retain water. As it loses water, it's capability to apply a hydrostatic pressure diminishes. The loss of water in the nucleus leads to a loss of elastin in the annulus fibrosus and disrupts the natural orientation of the collagen fibers [24]. A severe limitation in the extracellular

matrix's ability to distribute the load is a result. Without the hydrostatic pressure providing support and the extracellular matrix failing to properly handle the load, the disc loses height and the annulus fibrosus is allowed to expand outward, or "bulge", as it experiences compressive forces. In this situation, the compressive load acts unevenly on the annulus fibrosus, increasing the chance of injury. The risk of injury only increases with age as the nucleus pulposus becomes more dehydrated [27].

Alternatively, the hydrostatic pressure may diminish from a direct degradation of the vertebral end plates. People suffering from osteoporosis or vertebral compression fractures are likely to have weakened end plates. This allows for the nucleus pulposus to expand into regions typically filled by the end plates, increasing the total volume that the nucleus pulposus occupies. This increase in volume creates a drop in disc pressure, allowing for the bulging of the annulus fibrosus [9].

More severe and/or traumatic cases of Degenerative Disc Disease may lead to herniation of the nucleus pulposus through the annulus fibrosus. Herniation of the nucleus pulposus through the annulus fibrosus causes radial pain in the spinal region, largely attributed to the inflammatory response to the tissue. This pain is often localized to the affected disc, but in some cases, it can result in neural dysfunction [8]. This happens if the nucleus pulposus occupies the same space as the spinal cord or nerve roots. In the past, this has largely been attributed to a compressive force on the nerve from both the foreign tissue and inflammatory response, however more recent studies have shown that substances secreted from the nucleus pulposus alone are able to cause a neural dysfunction chemically. This mechanism is not yet fully understood, but some data suggest that TNF *a* is the primary contributor to this [26]. Even if the compressive force

is removed from the nerve and no disc tissue is coming into direct contact, leftover nucleus pulposus material may cause adverse effects on the spinal cord and nerve roots.

With degeneration also comes a loss of stability in the spine. This loss of stability has been linked to Osteophytosis, also known as bone spurs. It is theorized that the formation of bone spurs is the body's attempt to provide structure and compensate for the loss of mechanical function in the disc. Osteophytosis is most commonly observed in patients who had transdiscal tears [27][37].

Studies have shown that problems with the vascular system can lead to increased degeneration of the disc. With the annulus fibrosus and the nucleus pulposus being avascular tissues, the small nutrient supply they have is especially important. Vascular and cardiac disease, which become increasingly prevalent with age, can have serious downstream effects on the disc's nutrient supply. A small reduction in the function of these systems can essentially starve the disc. One study documented a drop in neuropillin-1 with increased age in rats. Neuropillin-1 regulates VEGF-induced angiogenesis. This correlates with another study showing a significant decrease in neuropillin-1 in human degenerated discs [38]. A separate study has shown that knocking out apolipoprotein E in rabbits is able to induce premature degenerative disc disease. Apolipoprotein E is essential in the regulation of cholesterol and triglycerides. By knocking out this protein, there is a much higher rate of progression of atherosclerosis. When examining the intervertebral discs in these animals, the treated rabbits all shown increased levels of disc degeneration. Cell viability in the test group was also much lower than the wild type as well as glucose levels in the tissue [39].

2.4. Clinical Treatment Options

2.4.1. Physical Therapy

The first step towards managing degenerative disc disease is typically a conservative route that includes various physical treatments. Exercise, application of heat/ cold, electrical stimulation, massage therapy can all be used to relieve pain without the need for surgery. Exercises promoting core strength specifically can help alleviate loads present in the spine [40]. Specific therapy programs will vary patient to patient, but it is typical for them to develop an at home routine that will focus on core, flexibility, and posture. Doing this will help properly distribute loads across the spine and may reduce pain [41].

Results of physical therapy tend to be similar regardless of the specialty of the prescribing physician, suggesting that variances in physical therapy programs do not have a large impact on delaying surgical interventions. However, early detection of degenerative disc disease increases the effects [42].

Exercise tends to be the most effective form of physical therapy. While techniques such as traction, massage, heat/cold may provide small amounts of immediate pain relief, its effects are short lived. When compared to core building, stabilization exercises, pain relief is similar immediately after treatment. However, exercise shows continued pain relief up to 12 months out [43].

2.4.2. Spinal Fusion

Spinal fusion surgery involves fixing two vertebrae together to prevent motion in that segment. Typically, a bone graft or scaffold is inserted into the diseased disc tissue to promote bone growth between the vertebrae and provide proper spacing [44]. A fusion

cage is attached using screws to fixate the vertebrae. There are a multitude of techniques for achieving this including anterior, posterior, and lateral approaches. Different approaches may be used in specific cases dependent if there are anatomical deformities, but in general surgeons tend to prefer using the technique they were trained with. Patient outcomes are similar between anterior and posterior approaches. Lateral approaches have been shown to provide a greater increase in spine stability [45].

Spinal fusion should only be performed in cases of motion based back pain, and even then its results are limited [44]. Spinal fusion may provide immediate pain relief in cases where the anatomy is pressing on the spinal cord, nerve roots, or muscles causing pain and/ or inflammation. However, it has been shown to not provide relief in non-specific lower back pain. A 2005 study of 349 patients (176 surgical group, 173 rehabilitation group) showed only a 4% difference in disability scores between a surgical and rehabilitation groups after 2 years. 19 patients had complications during surgery and 11 had reoperations [46]. Another study consisting of 124 patients showed at a 4 year follow up there was no significant difference between pain or disability in a surgical versus an exercise group. The number of patients in the exercise group who eventually did get surgery during the 4 years was similar to the number of reoperations in the surgical group, 24% and 23% respectively. Although, regular use of pain medication was significantly lower in the exercise group, 35% compared to 58% [47]. Spinal fusion also shows no benefit compared to stabilization surgery without fusion [48].

2.4.3. Total Disc Replacement

Total disc replacement involves replacing the diseased disc with an artificial one that can be made out of either metal or a metal and polymer combination. A surgeon will

approach the spine anteriorly, moving aside vital blood vessels and organs. Once there is access to the spine, the diseased disc is removed and replaced with the disc replacement [49]. A total disc replacement offers pain relief while preserving motion of the spine. Because of this total disc replacement is only viable for certain types of disc pathologies [50]. Typically it is more applicable to more moderate cases that do not involve compression of the nerve roots, and where pain is isolated to one or two discs [49].

Even though total disc replacement is supposed to have the benefit of maintaining motion, pain and disability scores of patients who receive total disc replacements are not significantly different from those who received spinal fusions [51]. Given the similar surgery approaches, complications between the two tend to be similar. This is demonstrated by a similar rate of adverse effects between total disc replacements and spinal fusions [52].

Total disc replacement is shown to improve VAS pain scores by 61% on average and an improvement of 25.8 points on the Owestry disability index over the course of 3 years. The 5 year clinical success rate of total disc replacements is around 58% [53]. This is comparable to spinal fusion surgery, however total disc replacements have shown about 1/3 the reoperation rate as spinal fusion surgery at a 7 year follow up [54].

2.4.4. Nucleus Pulposus Replacement

Nucleus Pulposus replacement devices aim to replace one specific part of the disc and restore function, instead of replacing the entire disc and limiting motion. While the primary endpoint of these devices is still to alleviate pain, their designed to mimic the biomechanics of the native tissue. Polymers and hydrogels are the typical material used in these cases [12]. These can better mimic the mechanical properties of the native tissue

and even replicate the tissue's ability to absorb water [55]. The material may be either preform or cure *in situ*. While preformed gels give greater control over the size, shape, and allow for a wider range of material use, *in situ* curing gels are less invasive and have a lower potential for expulsion [12].

The first prosthetic nucleus replacement device went into clinical trials in 1996. Various devices have gone through clinical trials since showing varying efficacy from 62% to 91% [55]. These devices have been proven to be able to hold up in the body and provide sufficient mechanical strength. One study showed that a void spinal disc will allow for inward bulging of the disc, while a sufficient nucleus replacement device is capable of preventing inward bulges with a modulus around 0.2 to 40 MPa [56]. Some devices may even be loaded with chondrocyte cells to promote growth of collagen matrix and healthy tissue, creating a regenerative approach. However, these approaches do not address the cause that started degeneration in the native tissue. Nutrient diffusion is still minimal in the disc area, making it hard for implanted cells to be successful [57].

Despite preforming similarly, if not better, to other surgical approaches, nucleus pulposus replacement devices see little use. Migration and expulsion of these devices is a large concern. These devices may also cause damage to endplates that they come into direct contact with, since weakened endplates are often associated with degenerative disc disease [55]. Studies have shown that nucleus pulposus replacement devices can be properly placed *in situ* and avoid migration, possibly making use of annulus closure techniques [58]. Regardless there is still hesitation from the medical community and the FDA. For a nucleus replacement device to become viable, it appears to require a significant increase in results compared to other surgical approaches.

2.5. PVA Based Hydrogels

2.5.1. Properties of Hydrogels

Hydrogels have seen increasing use in biomedical applications. A hydrogel is a combination material featuring hydrophilic polymer and water. Hydrogels are capable of absorbing large amounts of water and can be tailored to a have wide range of mechanical and biological properties. Because of this high water content, hydrogels are easily able to mimic soft tissue properties and can act successfully as a cell scaffold [59]. Hydrogels may be made from artificial or natural polymers. Reversible gels are the result of a physically crosslinked polymer network or secondary forces such has hydrogen bonding. Permanent gels are the results of covalent bonds forming within the network [60].

Dry hydrogel polymers are capable of absorbing anywhere from 10% their weight in water to a several thousand times increase. When water first enters the material, it will first be attracted to the most polar, hydrophilic groups of the polymer. As the material absorbs water, it will expand and expose hydrophobic groups. Water can become bound between these hydrophilic and hydrophobic groups until an equilibrium is reached [60]. Hydrogels may be tailored based on this swelling property. Hydrogels using larger polymers and with a higher number of cross links tend to have lower swelling rates and higher mechanical strength [61].

The first medical applications of hydrogels were wound dressings in the 1980s. Hydrogels are able to provide a scaffold for new cells to grow into as well as keep the tissue hydrated [59]. From there they showed great promise as soft contact lenses. Since then, hydrogels have expanded to having a wide range of applications, including tissue

engineering, drug delivery, cosmetic and hygiene products, and implantable devices [60] [61].

Mesh size and swelling properties largely dictate the properties of a hydrogel. These aspects of a gel can easily be controlled through methods that vary depending on the hydrogel polymer. These aspects may be manipulating using techniques such as thermal exposure, light exposure, pH, or chemical stimuli [62]. Mechanical strength of a gel should be similar to the tissue where the gel is being used. Water permeability and nutrient diffusion is dependent on mesh size of the hydrogel. This should be considered when designing a gel for a specific application [60].

2.5.2. Characteristics of PVA Based Hydrogels

Polyvinyl alcohol (PVA) based hydrogels show excellent biocompatibility and tunable properties. Mechanically, the response of PVA gels to force is rate dependent. This shows a viscoelastic property of the gel, which is expected. This is similar to the response of biological material under loading [63]. PVA gels may be prepared using physical or chemical cross links. Crystallites can form within the gel causing and increased mechanical strength in the gel. These crystallites may be increased inside the polymer matrix through the use of repeated freeze-thaw cycles. Gels that can have increased strength through freeze-thaw are sometimes referred to as cryogels [64]. PVA gels are also sensitive to pH, indicating the potential use for drug delivery applications [65].

Additional polymers may be added to PVA to create composite gels. These are favorable since they can take on the properties of multiple polymers [65]. One common polymer to use with PVA is polyethylene glycol (PEG). PEG acts as a physical cross

linker and porogen in PVA based gels [66]. PEG on its own has shown the ability to create aqueous osmotic swelling solutions on its own, where osmolarity increases with molarity [67]. PEG has been used in PVA based hydrogels to control swelling *in situ*, where levels of PEG can be adjusted to prevent significant swelling or dehydration within the body [68].

2.5.3. Crystallinity

Crystallinity is a naturally occurring process in PVA based gels, however it can also be induced through the use of freeze/ thaw cycles [64]. Freeze/ thaw cycles can be used to form stable crystalline structures within the PVA gel, however natural crystallinity from aging tends to be in a metastable phase. Improper cooling temperatures during freeze/ thaw cycles can lead to imperfect crystallinity growth [69]. Studies have shown higher levels of crystallinity in freeze/ thaw samples compared to natural aging. 30% and 35% PVA gels have shown a crystallinity of 3.59% and 5.20% respectively after 6 freeze/ thaw cycles. Comparatively, gels that have been aged 31 days showed 0.343% and 0.408% crystallinity at the same gel concentrations [70]. Another study showed a maximum crystallinity occurring after 7 weeks. This crystallinity is reversible through and autoclave process (121 °C) [17].

Chapter 3

Research Goals

The primary goal of this research is to determine conditions that allow for successful implantation of HYDRAFIL™ into the nucleus pulposus space and evaluate its ability to provide the proper biomechanics *in situ.* Thermal setting hydrogels, such as HYDRAFIL™, have varying viscosities and moduli at different temperatures. To ensure successful delivery of the gel, the gel must be held in a flowable state during injection through a delivery needle. Tests are developed to determine temperatures at which gelation occurs and what temperatures is crystallinity reversible.

Once the gel has reached the disc space, curing mechanics must be understood to ensure patient safety and prevent failure of the device. Evaluating gelation mechanics and expulsion conditions in recently injected hydrogels, recommendations can be developed on how avoid migration of the gel.

After fully setting in the body, the gel was evaluated for its ability to maintain hydration and restore biomechanics to the tissue. A successful implant should also integrate with the annulus fibrosus tissue. Mechanical loads, temperature control, and swelling solutions are all used to mimic conditions that would be found inside the body to develop an understanding of how the gel might behave *In situ.*

These goals are summarized in the research aims below:

Specific Aim 1: Characterize conditions that allow flow of HYDRAFIL™ and investigate effects of age and storage conditions on injection.

Specific Aim 2: Characterize curing behaviors under body conditions and develop recommendations for safe delivery.

Specific Aim 3: Investigate HYDRAFIL's™ capability to restore biomechanics and ability to integrate with the tissue.

Chapter 4

Injection Mechanics and Delivery Optimization

4.1. Introduction

Injectable hydrogels are used in biomedical applications due do their low invasiveness and tunable properties. In order to successfully deliver hydrogel to the treatment site, gels must be flowable through a reasonably sized needle; spinal needles typically range from 16-30 gauge, and not migrate from the delivery site [71]. Hydrogels can be designed to cure *in situ* through either physical or chemical crosslinks. Thermosetting gels make use of physical cross links to stiffen the hydrogel at a specific temperature [16].

For these methods, HYDRAFIL™, a cryogel used as a nucleus replacement device, was evaluated to determine under what conditions the gel is flowable. HYDRAFIL™ is injected into spinal discs through a 17 gauge needle and forms a contiguous implant when cooled to body temperature. The intention of the implant is to restore the biomechanics of the tissue and alleviate pain [72].

When heated above gelation temperature, gelation should be reversed and allow for HYDRAFIL™ to flow again. However, storage conditions and time may effect structural changes in the gel, such as the development of crystalline structures, that may add to the stiffness of the gel and decrease or prevent flow. If stiffness becomes too high, injection of the gel may be prevented. To ensure injectability, a method for reversing gelation and crystallinity must be developed.

For thermosetting gels, heat may be use reverse gelation and crystallinity. Researchers have previously used autoclaves to melt similar gels [17]. To ensure melting of crystalline structures, differential scanning calorimetry (DSC) will be implemented to measure the energy require melt crystalline structures and ensure a defined autoclave cycle is capable of accomplishing this. By using the DSC to mimic the proposed autoclave cycle, the amount of crystallinity melted in a gel sample by an autoclave can be quantified. Running an additional heat cycle beyond the range of the autoclave will detect any leftover crystallinity from the autoclave cycle [73].

Hydrogels cure *in* situ through the formation of non covalent bonds in a process called gelation. In order for a gel to be injectable, gelation must not yet have occurred [16]. Rheology will be used to determine under which conditions gelation happens. Rheology can determine a storage and loss modulus for a hydrogel. As the storage modulus increases relative to the loss modulus, the solid properties of the material increased. When the storage becomes greater than the loss, the hydrogel has reached gelation [74].

4.2. Methods

HYDRAFIL™ was prepared for use through a 30 minute 121°C steam autoclave cycle using a Tuttnauer 2540 autoclave. Gel was put into the autoclave inside of injection devices provided by ReGelTec. After autoclaving, gels were held at 65°C in a hot water bath until use.

Crystallinity was measured through a TA DSC 2500 using a heat-cool-heat cycle. The first heat cycle mimics the autoclave cycle (5.5°C/min ramp to 121°C, 15 minute

isothermal step), then a cool (-5.5°C ramp to 40°C), followed by a 2nd heat cycle to a higher temperature (5.5°C/min to 250°C).

Storage and loss moduli were measured using a TA Discovery Hybrid Rheometer 2. Gel was applied to the rheometer while flowable onto a 20mm crosshatch geometry. Tests were run at 2% strain, 1 hz, 1mm gap height.

4.2.1. Crystallinity Reversibility

Crystallinity was measured by the melt enthalpy required to completely melt crystalline structures within a sample. To observe the autoclave's ability to reserve increasing levels of crystallinity, a TA Instrument's DSC 2500 was used to mimic a 121°C autoclave cycle and then preforms a 2nd heat cycle to 250°C to ensure no additional melt events occur above 121°C.

HYDRAFIL™ for this test was divided into three test groups. A control, 3 freeze/ thaw cycles, and 6 freeze/ thaw cycles. At the beginning of the test, a bulk amount of hydrogel was autoclaved at 121°C for 30 mins in a Tuttnauer 2540 autoclave. Immediately after autoclaving, control samples were taken from the bulk gel and placed into high volume hermetic sealing DSC pans. The bulk gel then undergoes 3 freeze and thaw cycles. Each freeze thaw cycle, the gel was held at -20°C for at least 1 hour and then room temperature also for at least 1 hour. After the 3 freeze/ thaw cycles, samples were collected into DSC pans for the first test group. The bulk gel then undergoes an additional 3 freeze/ thaw cycles and samples were collected for the second test group.

Samples were heated at a rate of 5.5°C/min from idle (40°C) to 121°C, held isothermally for 15 minutes, cooled at the same rate back to idle temperature, held for an additional 15 minutes isothermally, and then heated at the same rate to 250°C.

Results are shown J/(g*s) vs time and J/(g*s) vs temperature. By integrating the melt curves in the J/(g*s) vs time graphs, a melt enthalpy can be acquired. Melt temperatures can be acquired by observing the temperature where the heat flow reaches a peak in the crystallinity melt curve.

4.2.2. Aging (Stored Gels)

Crystallinity for aged hydrogels can be determined using the same method as section 4.2.1. Samples were separated into three groups, a control group, a shelf aged group, and a swelling aged group. The control group are samples of freshly made gels, 5 days since their last autoclave cycle. The shelf aged group consists of gels stored in their injection devices at room temperature for over one year. The Swelling Aged group was formed into swelling samples of approximately 1 gram in weight. They were then secured in dialysis bags and submerged in an osmotic swelling solution designed to mimic osmotic pressure expected in the body. The swelling solution was created by mixing 128.2 grams of PEG 20k and 8.76 grams of NaCl into 1 liter of DI H20. Samples were stored for over 8 months at 37°C.

A TA Instrument's DSC 2500 was used to mimic a 121°C autoclave cycle and then preforms a 2nd heat cycle to 250°C to ensure no additional melt events occur above 121°C. Samples were heated at a rate of 5.5°C/min from idle (40°C) to 121°C, held

isothermally for 15 minutes, cooled at the same rate back to idle temperature, held for an additional 15 minutes isothermally, and then heated at the same rate to 250°C.

Results are shown J/(g*s) vs time and J/(g*s) vs temperature. By integrating the melt peaks in the J/(g*s) vs time graphs, a melt enthalpy can be acquired. Melt temperatures can be defined as the peak of the melt enthalpy curve in J/(g*s) vs temperature graphs.

4.2.3. Gelation (Temperature)

Gelation temperature is the temperature at which gelation occurs. This was measured using a TA hybrid rheometer. Tests were preformed using a 20 mm cross hatch geometry and base plate with a 1mm gap. The strain rate was 2% and a frequency of 1 hz. Storage and loss moduli vs time were measured. Gelation occurs when the storage modulus becomes greater than the loss [74].

Prior to the test, samples were heated in a 121°C autoclave cycle within the injection devices. Devices were then transferred to a hot water bath held at 65°C. After allowing device temperature to equilibrate to the water bath, approximately 0.31 mL of hydrogel was dispensed onto the base plate from the injection device. The geometry was lowered to the trim gap, excess material was removed, a solvent trap was placed around the testing geometry, geometry was lowered to geometry gap and the test begins. Peltier plate was set to 65°C before the start of test and during placement of sample. Machine will ramp to test temperature at the beginning of test.

4.2.4. Statistics

Results for crystallinity reversibility and aged crystallinity were evaluated for significance using a one-way ANOVA. This was followed by a Tuckey's post hoc test with a 95% confidence interval.

4.3. Results

4.3.1. Crystallinity Reversibility

Small amounts of crystallinity were observed in gels over a relatively short storage time (5-6 days, see column 2 in ***Table 1*** below). Increased crystallinity is observed with increased freeze/ thaw cycles, similar to results shown in other works. Samples with no freeze thaw cycles had an average melt enthalpy of 1.46 J/g. Melt enthalpy significantly increased ($p<0.5$) to 4.40 J/g and 5.26 J/g for 3 and 6 freeze/ thaw cycles respectively (***Figure 1***).

Crystallinity was shown to be completely reversible during a 121°C autoclave cycle. No melt events were observed in any sample during 2nd heat cycle (Pink line in ***Figure 5***).

Table 1

Crystallization Melt Enthalpy and Temperature with Freeze Cycles

Sample Name	Days since autoclave	Freeze Cycles	Melt Peak Temperature (°C)	Crystallization Melt Enthalpy (J/g)
Control 1	5	0	99.61	1.953
Control 2	5	0	94.93	2.361
Control 3	6	0	102.79	1.354
Control 4	6	0	100.60	0.187
3 Freeze/Thaw 1	5	3	106.56	4.221
3 Freeze/Thaw 2	5	3	102.22	4.583
6 Freeze/Thaw 1	6	6	101.78	4.127
6 Freeze/Thaw 2	6	6	101.99	6.403
Average Control	5.5	0	99.48	1.464
Average 3 Freeze	5	3	104.39	4.402
Average 6 Freeze	6	6	101.89	5.265

Figure 1

Statistical Comparison of Frozen Groups

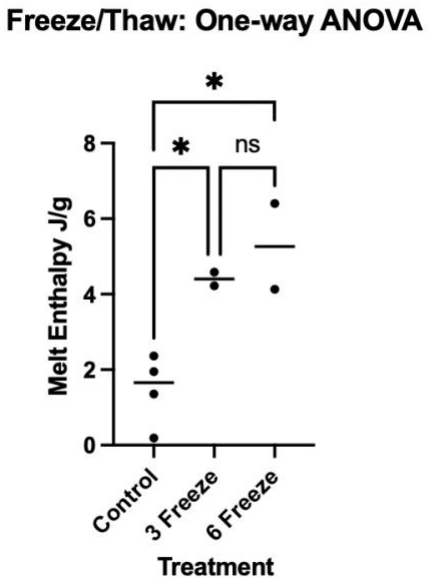

*Note. *=p<0.05, **=p<0.01, ***=p<0.001, ****p<0.0001*

Figure 2

Control Sample 3 - Crystallinity Melt Enthalpy

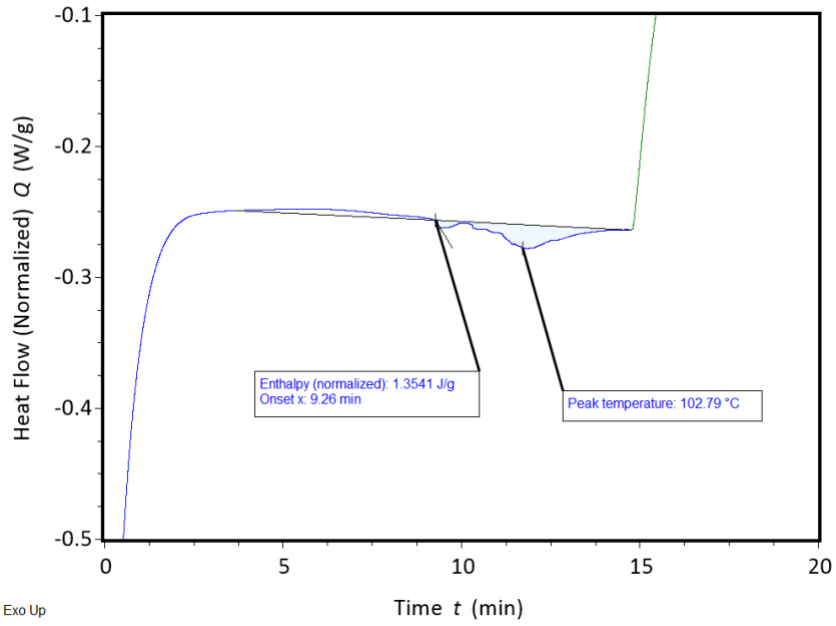

Note. Control Sample 3 displayed a melt enthalpy of 1.354 J/g with a melt temperature of 102.79°C six days after the last autoclave cycle.

Figure 3

3 Freeze/Thaw Sample 2 - Crystallinity Melt Enthalpy

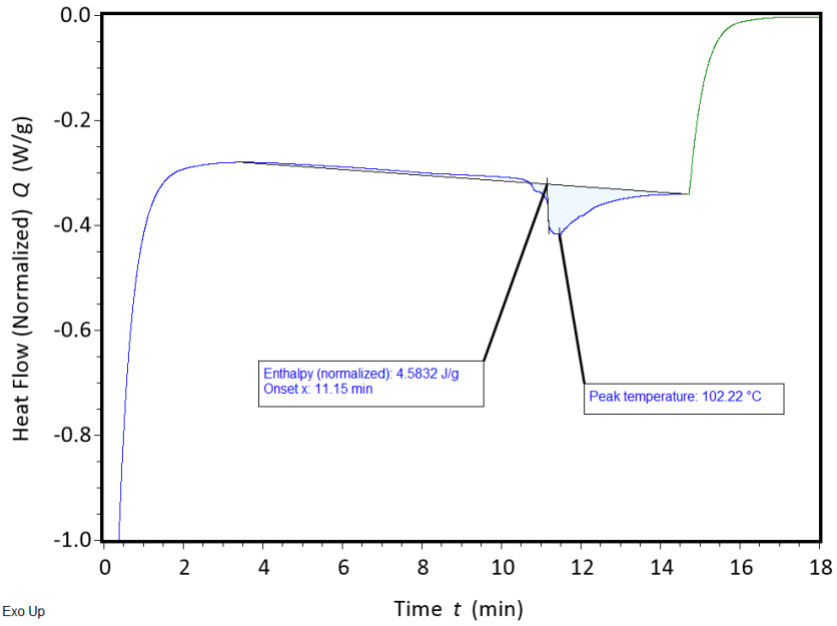

Note. 3 Freeze/Thaw Sample 2 displayed a melt enthalpy of 4.583 J/g with a melt temperature of 102.22°C five days after the last autoclave cycle.

Figure 4

6 Freeze/Thaw Sample 2 - Crystallinity Melt Enthalpy

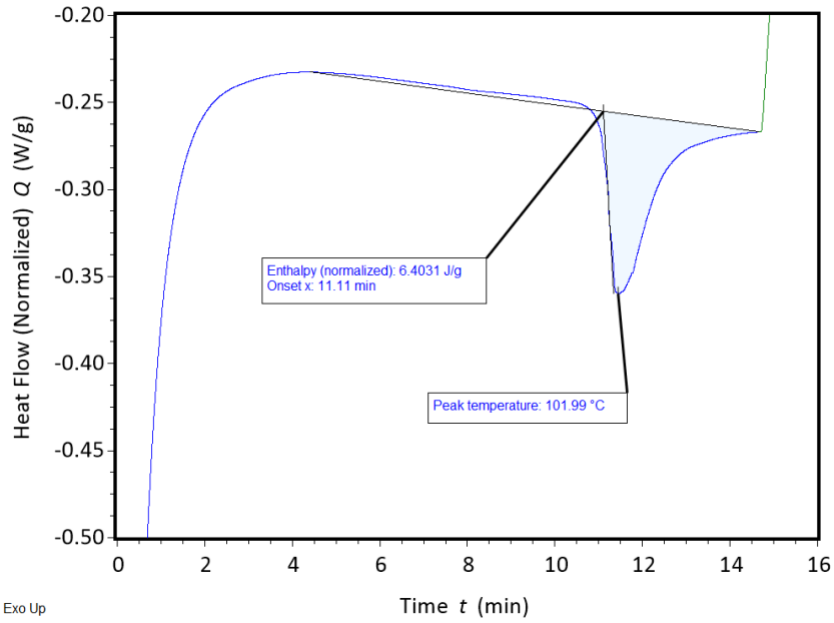

Note. 6 Freeze/Thaw Sample 2 displayed a melt enthalpy of 6.403 J/g with a melt temperature of 101.99°C six days after the last autoclave cycle.

Figure 5

Heat Flow vs Temperature – 6 Freeze/Thaw Sample 2

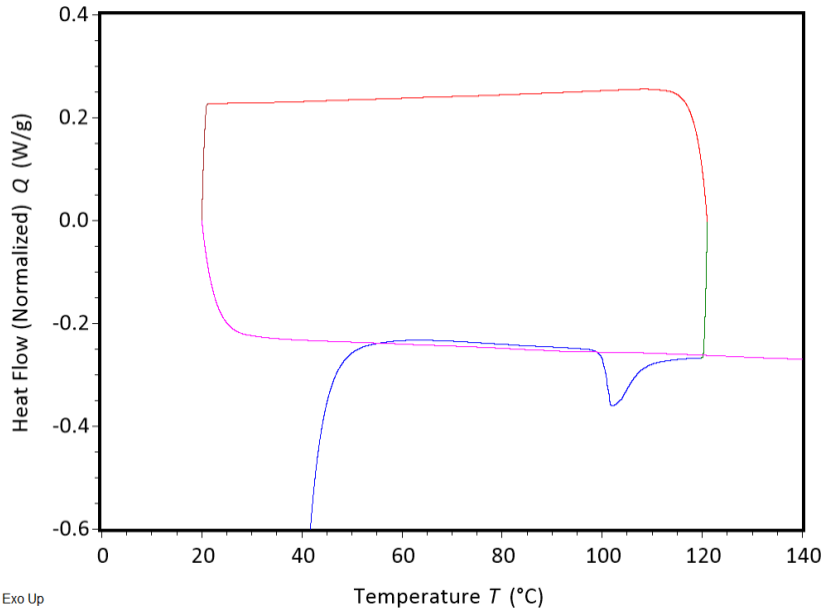

Note. First heat ramp is in blue, cooling cycle is in red, second heat ramp is in pink.

4.3.2. Aging (Stored Gels)

Gels demonstrated significantly increasing crystallinity with time ($p<0.007$). Gels in the control group, only aged 5 days, showed similar results to the control group in section 4.3.1 with an average crystallinity melt enthalpy of 2.92±0.077 J/g . Crystallinity increases to an average of 9.90±1.12 and 11.31±0.813 J/g for shelf aged and swelling aged samples, respectively (***Figure 6***).

Melt temperature for the control group was also similar to previous results at 99.03°C on average. Melt temperature dropped for aged samples to 92.28 and 82.90°C for shelf aged and swelling aged respectively. No additional melt events were observed after the mimic autoclave cycle in any sample (pink line ***Figure 9***).

Figure 6

Statistical Comparison of Aged Groups

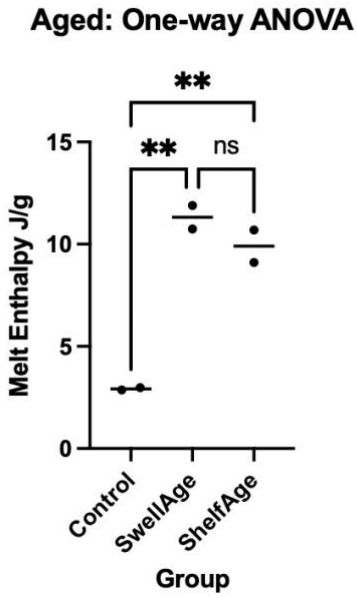

*Note. *=p<0.05, **=p<0.01, ***=p<0.001, ****=p<0.0001*

Table 2

Crystallization Melt Enthalpy and Temperature with Age

Sample Name	Age	Melt Peak Temp (°C)	Crystallization Melt Enthalpy (J/g)
Control 1	5 Days	95.06	2.98
Control 2	5 Days	102.99	2.87
Shelf Aged 1	1 year+	91.87	10.70
Shelf Aged 2	1 year+	92.68	9.11
Swelling Aged 1	8 Months	80.93	10.74
Swelling Aged 2	8 Months	84.86	11.89
Average Control	5 Days	99.03	2.92
Average Shelf Aged	1 year+	92.28	9.90
Average Swelling	8 Months	82.90	11.31

Figure 7

Control Sample 1 - Crystallinity Melt Enthalpy

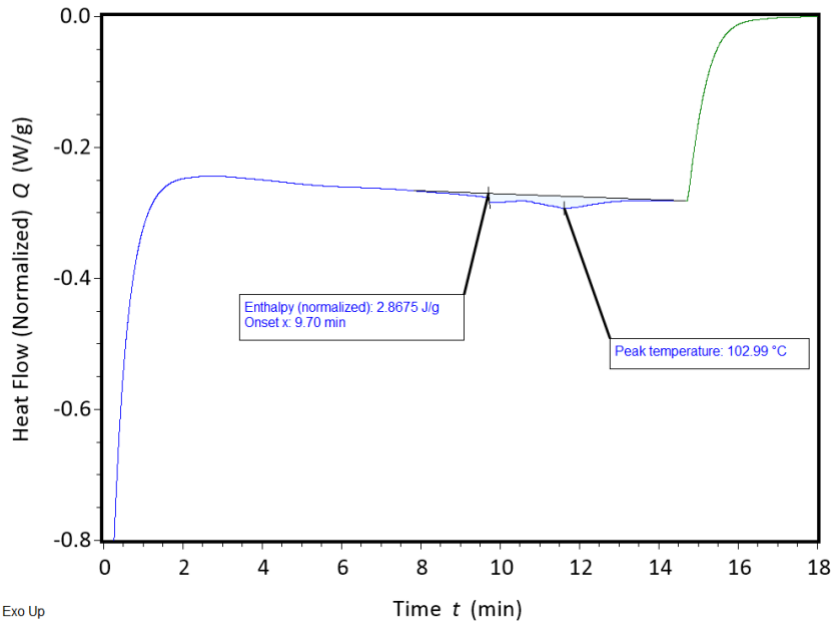

Note. Control Sample 1 displayed a melt enthalpy of 2.868 J/g with a melt temperature of 102.99°C five days after gel synthetization.

Figure 8

Shelf Aged Sample 1 - Crystallinity Melt Enthalpy

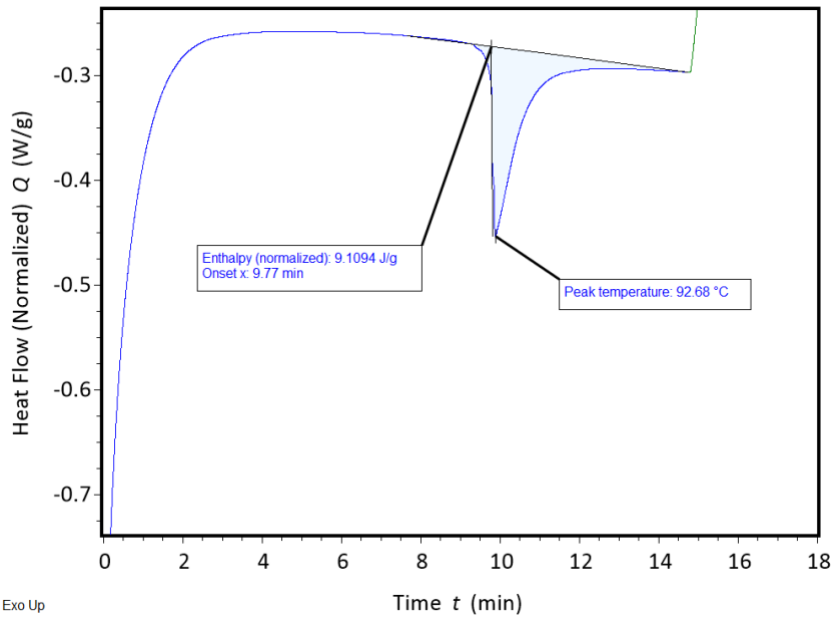

Note. Shelf Aged Sample 1 displayed a melt enthalpy of 9.109 J/g with a melt temperature of 92.68°C after more than 1 year of storage inside the injection device at room temperature.

Figure 9

Heat Flow vs Temperature – Swelling Aged Sample 1

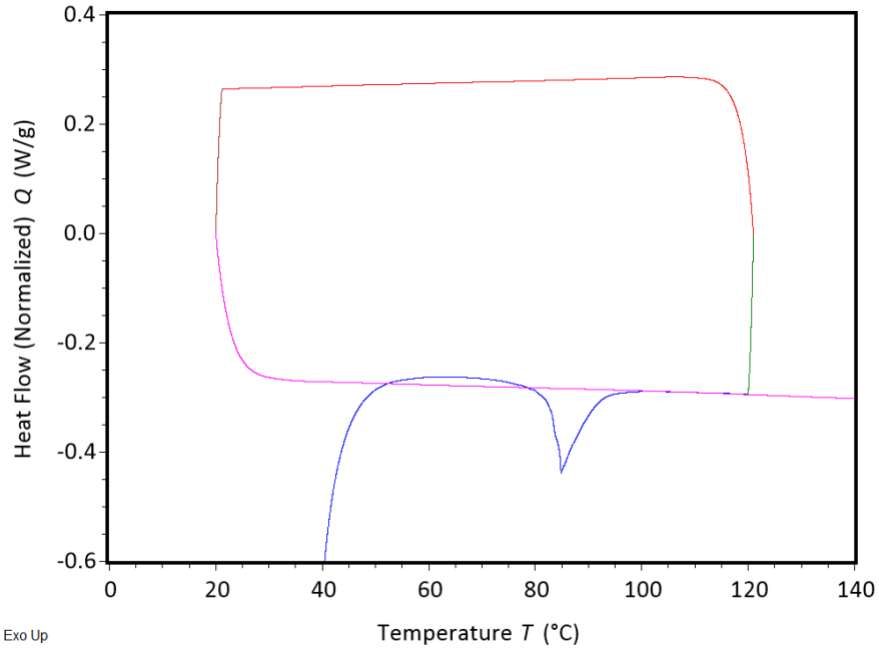

Note. First heat ramp is in blue, cooling cycle is in red, second heat ramp is in pink.

4.3.3. Gelation (Temperature)

After a 30 minute autoclave cycle (121°C), no gelation was observed at 65°C for a prolonged period of time. Gel was tested shortly after autoclaving, allowing time for the gel to equilibrate at the test temperature. Storage and loss moduli were collected from the rheometer (***Figure 10***). Bulk gel was held at the test temperature of 65°C for 24 hours to ensure that gelation doesn't occur over a longer timeframe. No gelation was observed after 24 hours and the sample displayed similar storage and loss moduli to the previous test (***Figure 11***).

At 62°C gelation was undefined. Storage and loss moduli converge after a few minutes and there was no clear overlap of one over the other (***Figure 12***). Gelation was

observed at 60°C. HYDRAFIL™ reached gelation after 746 seconds at the set temperature (***Figure 13***)

Figure 10

Gelation Temperature 65°C

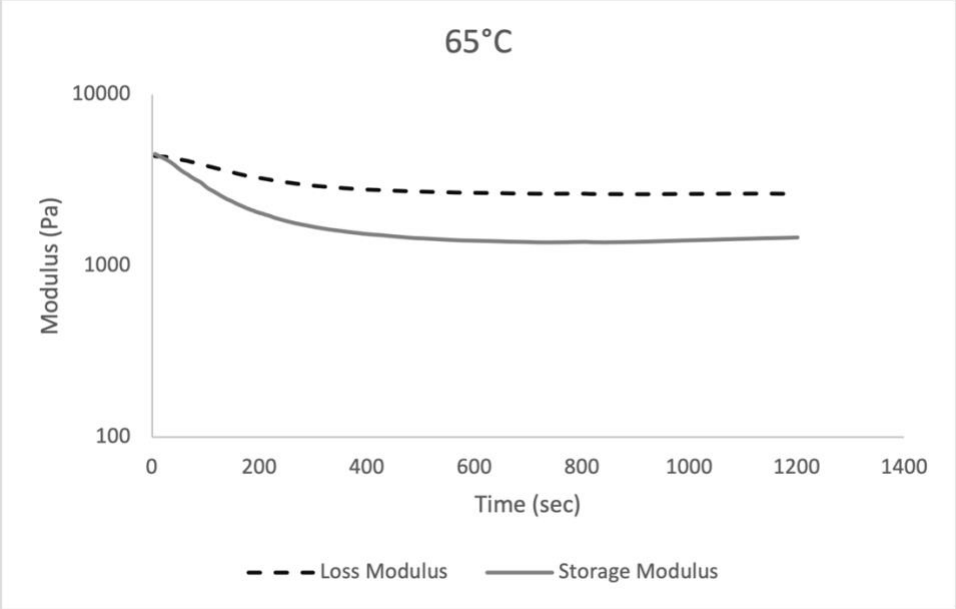

Note. No Gelation Was observed at 65°C

Figure 11

Gelation Temperature 65°C - 24 Hour Isothermal

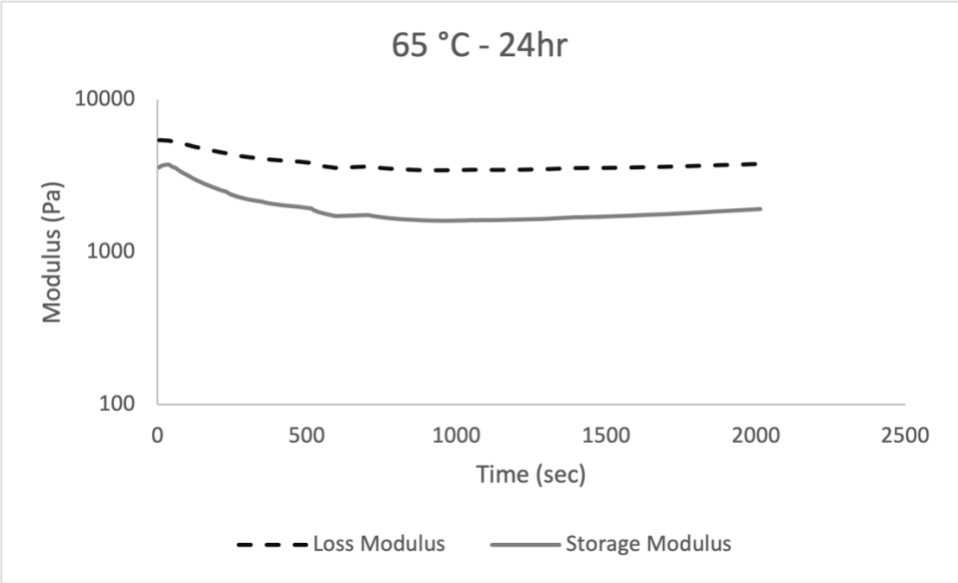

Note. After autoclaving, gel was held at 65°C inside the injection devices using a hot water bath for 24 hours before testing.

Figure 12

Gelation Temperature 62°C

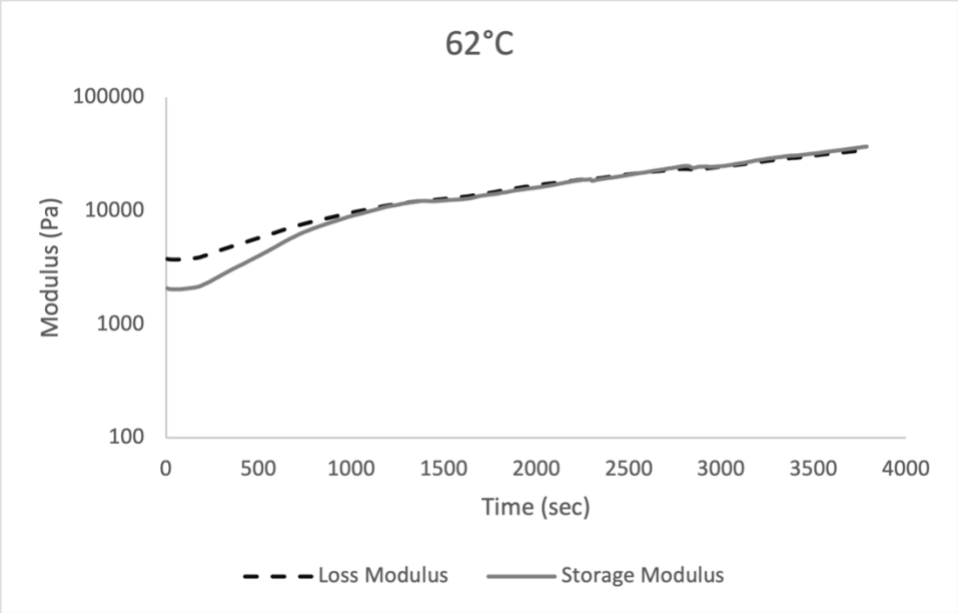

Note. There was no apparent gelation after 1 hour. Loss and Storage modulus converged and were colinear for an extended period of time.

Figure 13

Gelation Temperature 60°C

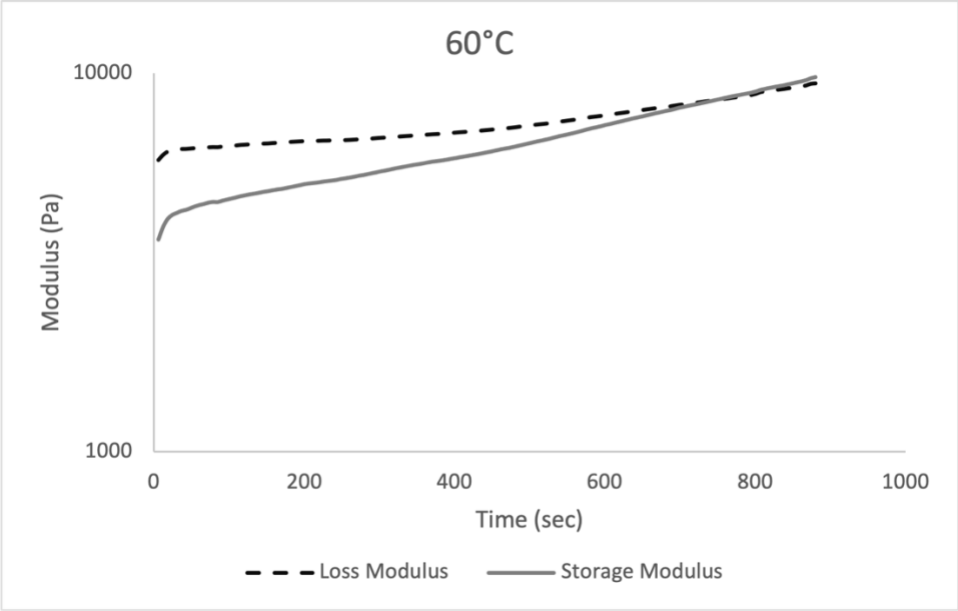

Note. Gelation was observed after 746 seconds at 60°C

4.4. Discussion

For successful delivery of the hydrogel, the gel must be flowable under the desired injection conditions. Thermally-setting hydrogels can have their gelation reversed through heat cycling. Gelation of this gel is the result of both physical cross links and crystallinity growth. To revert the gel to a flowable state, both the gelation and crystallization must be reversed.

Making use of an autoclave cycle, crystallinity and gelation were shown to be reversible. Crystallinity grows slowly over time under different storage conditions, but may be increased artificially through the use of freeze and thaw cycles, similar to previous studies [17]. In order to confirm melt events shown in DSC curves were in fact

crystallinity, gels were put through repeated freeze/ thaw cycles, and then ran through a heat-cool-heat cycle on the DSC. With increased freeze/ thaw cycles you would expect an increase in melt enthalpy.

Gels stored a short period of time (5-6 days) exhibited over a 3-fold increase in crystallinity when subjected to freeze/ thaw cycles. Gels with increased crystallinity can be used as a positive control to demonstrate injectability was still possible after extreme conditioning. Despite this increase, autoclaving the hydrogel has shown to reverse crystallinity in all samples.

Aged gels showed even greater crystallinity levels. The average 6 freeze/ thaw sample had a crystallization melt enthalpy of 5.27±1.61 J/g, while the shelf aged sample had an average crystallization melt enthalpy of 9.90±0.813 J/g.

Aged samples were split into two groups, shelf aged and swollen aged. Shelf Aged group represents the gel's characteristics and being held in typical storage conditions and gives insights to the shelf life of the hydrogel. PVA based hydrogels have been shown to increase in crystallinity over time. This increase in crystallinity both increases stiffness and reduces hydration of the gel. HYDRAFIL™ has been shown to have crystallinity reversed when using the proposed autoclave cycle.

Swollen aged samples were kept in an osmotic swelling solution at 37°C, mimicking the expected conditions the gel would face inside the body. These samples can be used to predict the behavior of the gel when its in the body. The melt temperature was at lower temperatures in the aged samples, going as low as 80.93°C in swelling aged sample 1 (***Table 2***), compared to the average control sample melt temperature of 99.03±5.61°C (***Table 2***). Crystallinity has been previously shown to increase phase

separation of water from the gel [70]. Swollen gels, despite high crystallinity values, maintain a low melt temperature. This is likely due to the swelling solution overcompensating for the water loss due to crystallinity. Increased water content increases flowability, including a lower melt temperature.

After reversing crystallinity, gels should be able to be held in a flowable state indefinitely as long as they are kept above the gelation temperature. After autoclaving, no gelation was observed at 65°C, even after 24 hours (***Figure 10*** & ***Figure 11***). Gelation was observed at 60°C after 746 seconds (***Figure 13***). At 62°C gelation was undefined, with neither the storage nor the loss clearly overtaking the other (***Figure 12***). Holding autoclaved gels above this temperature prevents crystallinity and preserves injectability.

Crystallinity in HYDRAFIL™ was shown to be reversible through the use of autoclave cycles. Once autoclaved, gels may be held above the gelation temperature indefinitely and still be injectable. HYDRAFIL™ should be held above 62°C to ensure gelation does not occur, but not so high that it may cause damage to the surrounding tissue.

Chapter 5

Short Term Mechanics of Hydrogel *In Situ*

5.1. Introduction

In order to effectively inject a hydrogel into a desired space, gelation and short-term mechanics of the hydrogel must be understood. Gelation will act as the primary resistance to expulsion. Once gelation has occurred the gel will no longer flow easily, requiring large amounts of force to displace the implant. Determining a sufficient amount of time before placing load on the implant is crucial to patient outcome, since expulsions can lead to failure of the implant or damage to the surrounding tissue.

To determine required cure times to prevent expulsion, gelation will be observed through the use of rheology as well as more practical experiments. Rheology will be used to determine the time that gelation occurs at body conditions [16]. Other tests will mimic conditions in the body through the use of temperature controls, surrogate annuli, and swelling solutions.

A surrogate annulus is a device for testing nucleus pulposus replacement technologies. The surrogate annulus was designed to mimic the physiology of the spine and made out of a material with a similar stiffness to the annulus fibrosus [75]. Static forces on annuli can be replicated through the use of mechanical testing devices.

Once in the body, to properly function as a nucleus replacement device, the gel must be able to equilibrate and swell to the proper hydration level for the osmotic pressure of the tissue [76]. This includes being able to recover from a dehydrated state that may be introduced due to storage conditions.

5.2. Methods

HYDRAFIL™ was prepared for use through a 30 minute 121°C steam autoclave cycle using a Tuttnauer 2540 autoclave. Gel was put into the autoclave inside of injection devices provided by ReGelTec. After autoclaving, gels were held at 65°C in a hot water bath until use.

Storage and loss moduli were measured using a TA Discovery Hybrid Rheometer 2. Gel was applied to the rheometer while flowable onto a 20mm crosshatch geometry. Tests were run at 2% strain, 1 hz, 1mm gap height. Complex modulus was measured on solid gels at 2% strain, 1 hz, and 2mm gap height.

Compressive force for expulsion was applied through the use of a Shimadzu EZ-X tensile tester. For short term expulsion testing a 450N load was applied at 25 N/sec at the specified test time.

5.2.1. Gelation (Time)

Gelation time is the time at which gelation occurs at a given set temperature. This was measured using a TA discovery hybrid rheometer 2. Tests were performed using a 20 mm crosshatch geometry and base plate with a 1mm gap. The strain rate was 2% and a frequency of 1 hz. Storage and loss moduli vs time were measured. Gelation occurs when the storage modulus becomes greater than the loss.

Prior to the test, samples were heated in a 121°C autoclave cycle within the injection devices. Devices were then transferred to a hot water bath held at 65°C. After allowing device temperature to equilibrate to the water bath, approximately 0.31 mL of hydrogel was dispensed onto the base plate from the injection device. The geometry was

lowered to the trim gap, excess material was removed, a solvent trap was placed around the testing geometry, geometry was lowered to geometry gap and the test begins. Peltier plate was set to 65°C before the start of test and during placement of sample. Machine will ramp to test temperature of 37°C at the beginning of test. Time until gelation occurs was recorded as well as time for the test to reach 37°C.

5.2.2. Expulsion

Expulsion tests were performed by injecting prepared hydrogel held at 65°C into a surrogate annulus. Surrogate annuli were created following ASTM standard [77]. Suggested dimensions for surrogate annuli are shown below in ***Figure 14***.

Figure 14

Suggested Design for Surrogate Annulus

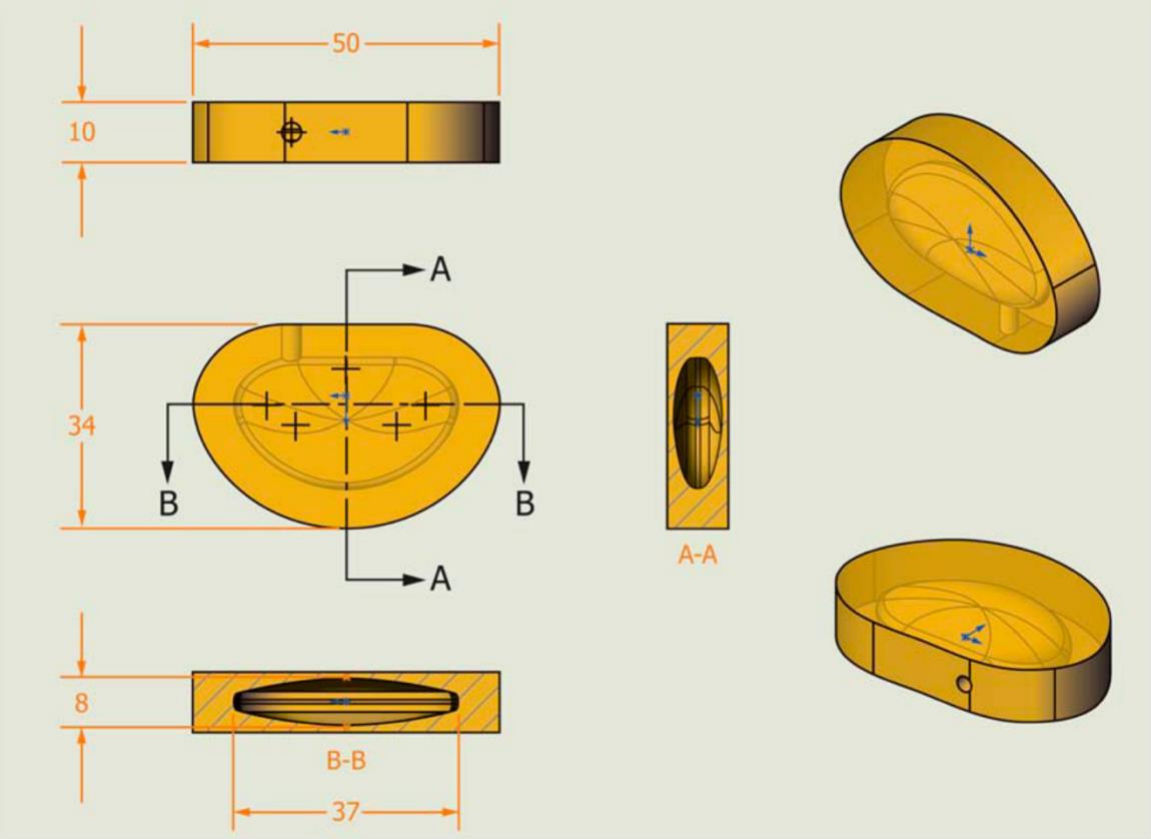

Note. Interior cavity for nucleus pulposus was reduced to 1.2 ml in final design

In order to create the surrogate annulus, a wax core representing the nucleus pulposus was injection molded using a split 3D printed mold (shown in ***Figure 15***). Once molded, the wax core was placed into the full surrogate annulus mold (shown in ***Figure 16***). The stem of the wax core extends radially to the edge of the annulus to create a pathway for the wax to escape. RTV 630 silicone resin was used to fill the annulus mold. After waiting 48 hours for the silicone resin to cure, the annulus was removed from the mold. Then annulus was then heated to melt the wax, and the wax was then drained

through the port created by the stem. The complete surrogate annulus is shown in ***Figure 17***. The port for the wax core was plugged using a quick setting silicone putty.

Figure 15

Mold for Wax Core

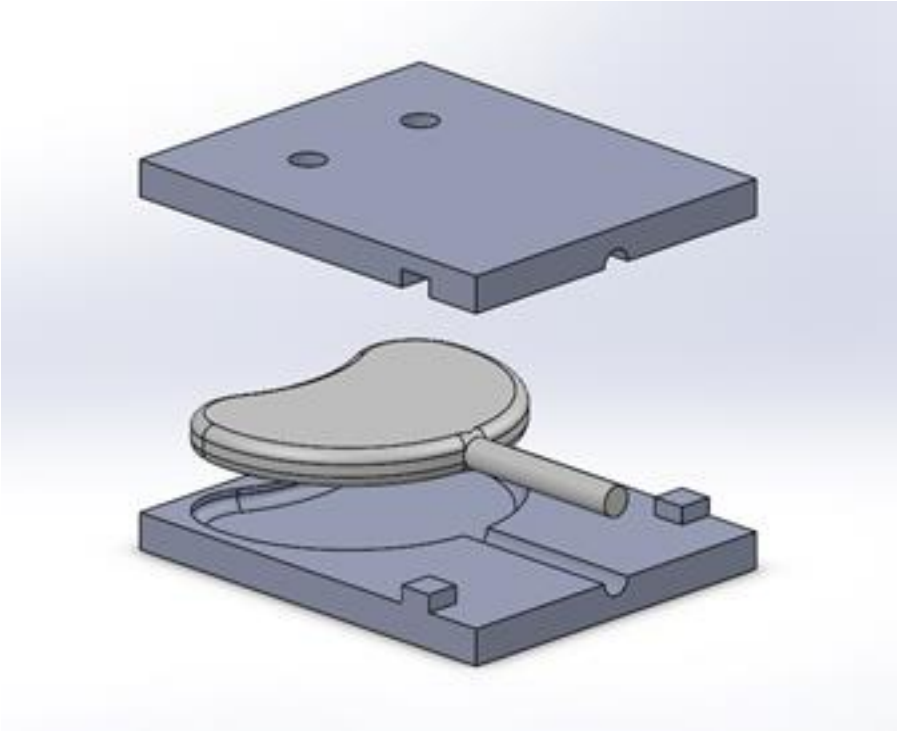

Figure 16

Surrogate Annulus Mold

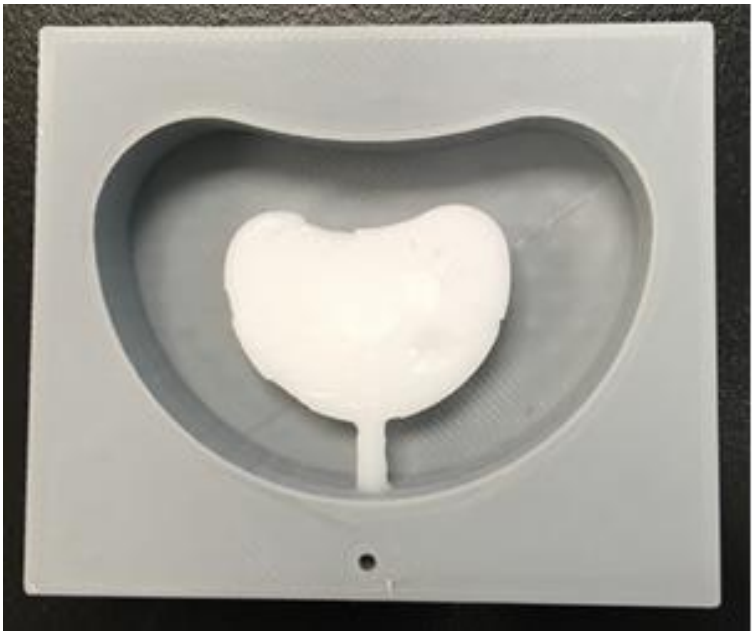

Note. Wax stem extends to the edge of the annulus mold

Figure 17

Surrogate Annulus

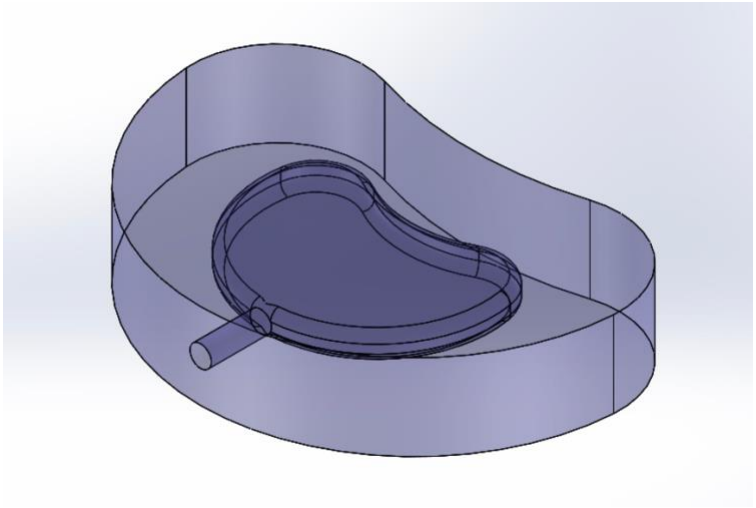

Note. Prior to use, port for wax core is plugged using a quick setting silicone putty.

A 17-gauge needle was introduced into the annulus laterally. Hydrogel was injected into the annulus until the cavity was filled. The injection device was removed from the needle and a trocar was introduced into the needle for the set time for the test. After the time has passed, the needle was removed and replaced with a 17-gauge port. A guide to putting the port in place was shown in ***Figure 18*** below.

Figure 18

Insertion of Expulsion Port

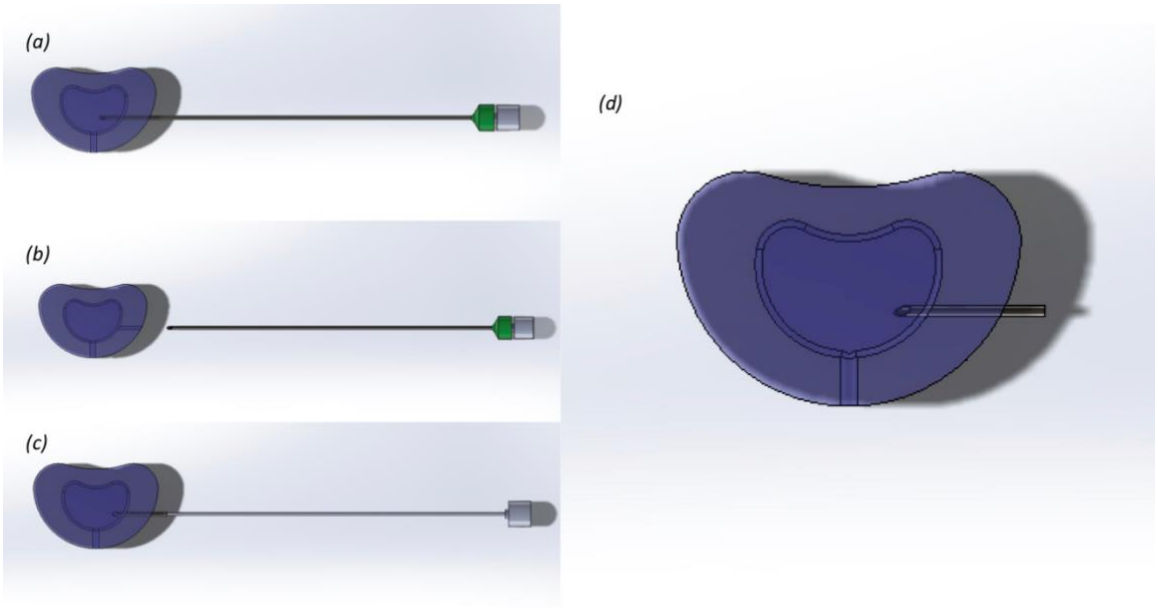

Note. (a) Needle inserted into cannula (already in place) after injection. (b) Needle and cannula removed from surrogate annulus. (c) 17G expulsion port and needle introduced into the same pathway the cannula was in. (d) Needle was removed leaving the 17G expulsion port in place.

With the port in place, the annulus was loaded onto a Shimadzu EZ-X mechanical tester. The disc was put under a compressive load of 450N at a rate of 25 N/s. If hydrogel was observed to come through the port, then the test has failed. Surrogate annulus injection and compression tests were performed at 37°C.

5.2.3. Hydration Recovery

To examine the gel's ability to regain hydration lost through phase separation during storage, gel samples were formed and then partially dried. After drying samples complex modulus were tested to look for changes in mechanical strength.

Freshly made hydrogel was formed into a 20mm diameter circular mold with a 2 mm height. Samples were separated into three groups. Group 1 was the control group with no additional conditioning performed to the samples. Group 2 was dried at room temperature in open air for 1 hour. Group 3 was dried at 37°C in open air for 1 hour.

All Samples were tested on a TA Instruments DHR 2 Rheometer. Tests were performed using a 20 mm crossed-hatch geometry under 5N of axial load. Tests were run at 2% strain and 1 hz. After testing, samples were submerged into an osmotic swelling solution created by mixing 128.2 grams of PEG 20k, 8.76 grams of NaCl, and 1L of DI H20. Samples were left in solution to swell for one week and then tested again.

5.2.4. Statistical Analysis

Results for hydration recovery were evaluated for significance using a two-way ANOVA. This was followed by a Tuckey's post hoc test with a 95% confidence interval.

5.3. Results

5.3.1. Gelation (Time)

Gelation time was measured as the time to gelation at 37°C. Out of 6 samples tested, gelation occurred after 292±165 seconds. It should be noted that Sample 1 was an outlier from the other results. This may the result of improper test set up. If this sample was excluded from the results, the average gelation time is 232±45 seconds with a notable drop variance. Average time to 37°C from the 65°C pretest temperature was 66 seconds. Sample 1 also had the shortest time to 37°C at 55 seconds. A typical result, sample 5, is shown below (**Figure *19***). Gelation times for all samples are shown in **Table *3***.

Figure 19

Gelation Time - Sample 5

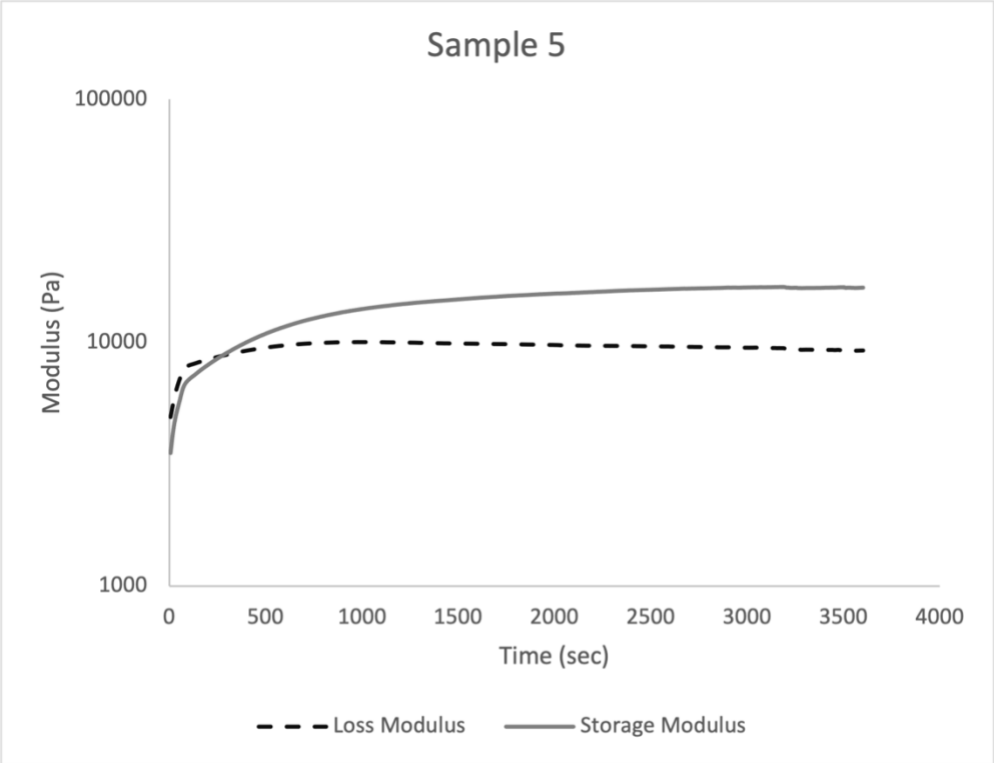

Note. Gelation was observed to occur after 273 seconds for Sample 5. It took 67 seconds for the sample to reach 37°C.

Table 3

Gelation Times - 37°C

Sample	Gel Time (sec)	Time to 37 (sec)
1	656	55
2	237	73
3	218	67
4	152	73
5	273	67
6	273	61
7	237	67
Avg	292	66
St Dev	165	6.4

Note. If sample one is excluded, average gelation time and standard deviation are 232 and 45 secs respectively.

5.3.2. Expulsion

Expulsion was no observed after 1 minute. One sample with a 5 minute set time was excluded from this data do an inconsistency with the other results. It is suspected that this sample expulsed because the hydrogel was still above 65°C from the autoclave, making it less viscous. Subsequent tests at 5 to 1 minutes showed no expulsion. Expulsion was observed at the 0 minute time point.

Table 4

Expulsion Times

Sample:	Set Time:	Result:	Weight (g):
1	10:00	Pass	1.24
2	9:00	Plug came out	n/a
3	9:00	Pass	1.21
4	8:00	Pass	1.20
5	7:00	Pass	1.00
6	5:00	Pass	1.27
7	4:00	Pass	1.22
8	1:00	Pass	0.99
9	1:00	Pass	1.05

5.3.3. Hydration Recovery

Samples were prepared in accordance with ***Table 5*** below. Dryness is the weight percent of water lost for each sample. Group 1 experienced no drying and on average Groups 2 and 3 had 25.3% and 60.2% dryness respectively.

Table 5

Drying Treatment by Sample

Group	Samples	Drying Temperature	Drying Time	Average Dryness
1	1-1, 1-2, 2-1, 2-2	n/a	0	0%
2	3-1, 3-2, 4-1, 4-2	Room Temp	1 hr	25.3%
3	5-1, 5-2, 6-1, 6-2	37°C	1 hr	60.2%

No significant increase in modulus was observed between groups 1 and 2, but a very significant increase in modulus for group 3 pre-swelling ($p<0.0001$). Post swelling there was no significant difference in modulus between groups (***Figure 20***).

Figure 20

Statistical Comparison Between Groups - Pre and Post Swelling

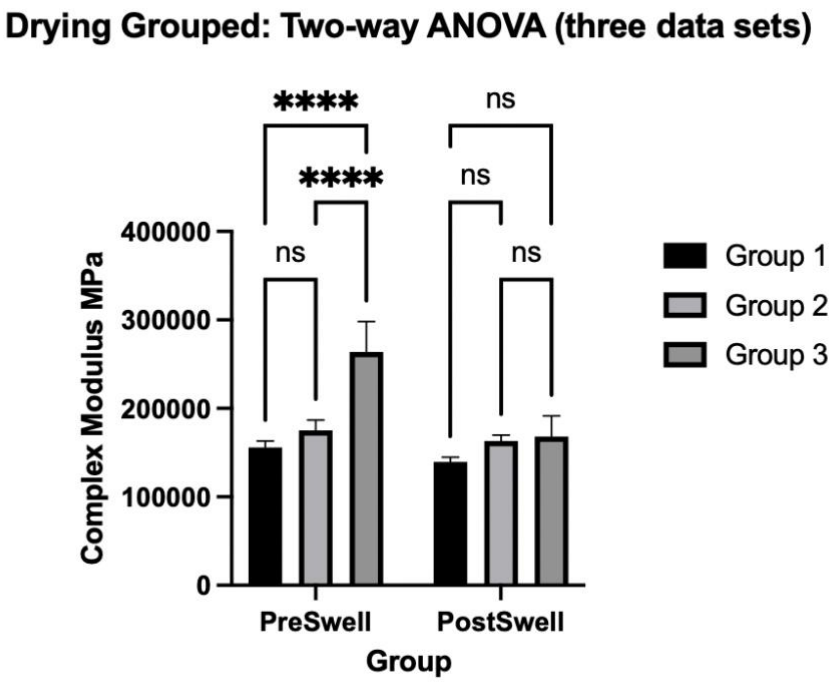

Note. *=p<0.05, **=p<0.01, ***=p<0.001, ****=p<0.0001

Figure 21

Modulus vs Dryness

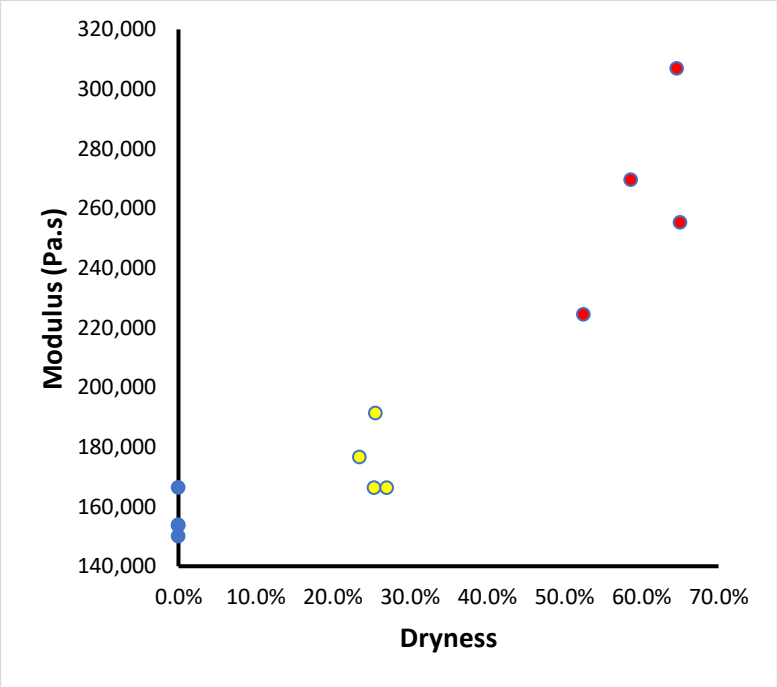

Note. Shown are Group 1 (blue), Group 2 (yellow) and Group 3 (red). Group 1 had no drying performed so all dryness values for group are assumed to be 0.

Figure 22

Modulus vs Weight – Pre Swelling

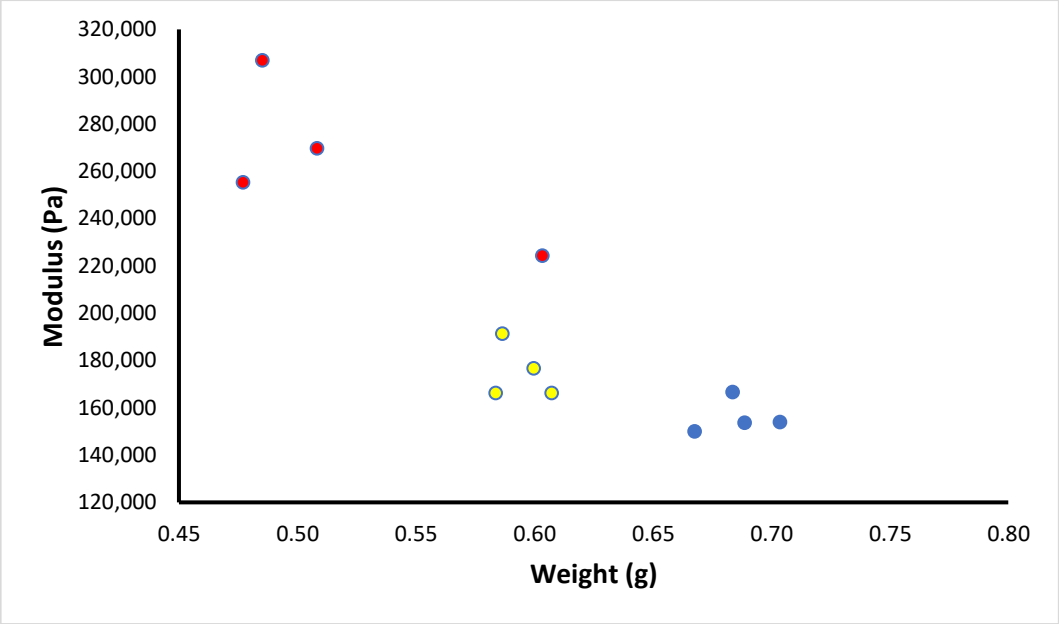

Note. Shown are Group 1 (blue), Group 2 (yellow) and Group 3 (red).

Figure 23

Modulus vs Weight - Post Swelling

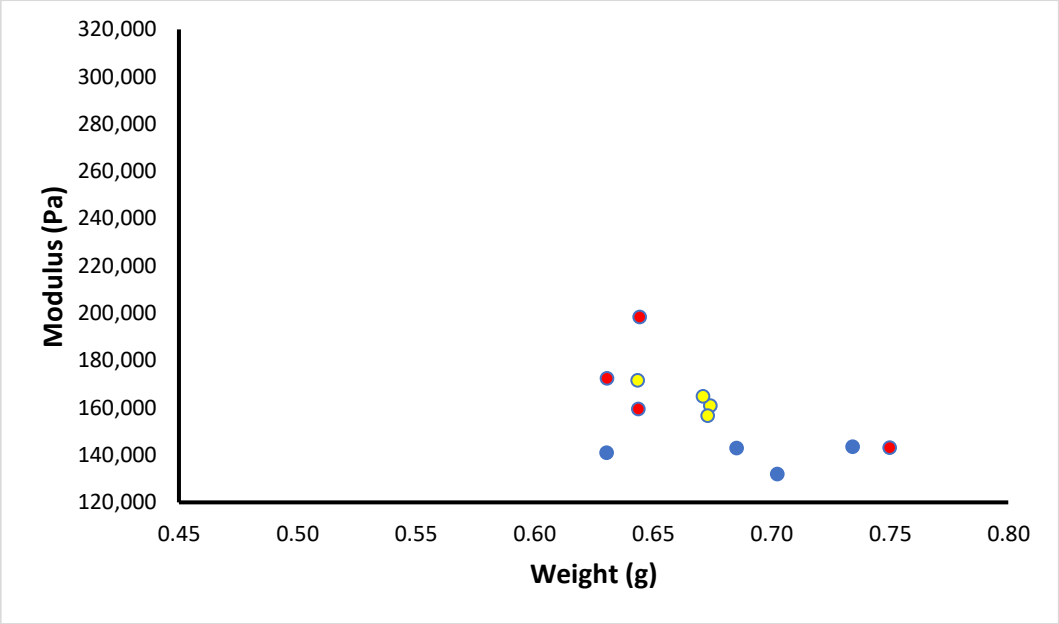

Note. Shown are Group 1 (blue), Group 2 (yellow) and Group 3 (red).

5.4. Discussion

To act as a successful implant, Hydrfil must be able to cure *in situ* under expected conditions, resist expulsion, and reach proper hydration levels in the body. The gelation mechanism of hydrogel helps prevent flow of the gel, but even before gelation occurs, the increasing stiffness of HYDRAFIL™ as it cools can be enough to prevent expulsion through small enough pathways. Once in the body, Hydrfil must be able to maintain proper hydration regardless of potential water loss during storage.

Gelation occurs after a few minutes at 37°C. On average samples gelled after 292±165 seconds. However, improper test set up may have caused additional moisture to fall on sample 1, elongated the time to gelation. If this sample was excluded from the data than the average gelation time is 232±42 seconds. Even though no observations were

made during the time of the test, the high variance introduced by sample 1 was more likely an error than a true result.

Expulsion was not observed after 1 minute of set time. The one excluded result was likely due to the gel still being above the hold temperature of 65°C, causing a decrease in viscosity. Following that test, all samples were allowed to set for at least 1 minute and did not have an expulsion through the expulsion port. Sample 2 (***Table 4***) did not have an expulsion through the expulsion port but did drive out the silicone plug blocking the path for the wax core, meaning the gel is able to flow through larger diameters. Given that gelation time from the previous section was determined to 232±42 seconds and you would expect some flowability before gelation. At set times between 60 seconds and the determined gelation time, gel is not expulsing because it can't flow, but rather the shear forces associated with traveling through a 17-gauge needle port are too large to allow flow outside of the surrogate annulus.

When injected into the body, the hydrogel will equilibrate with the interstitial fluids in the tissue. The hydrogel demonstrates and ability to recovery any lost hydration that may have happened during storage. Even in severe bench top cases where dryness was as high as 65%, the gel was able to reabsorb almost all lost water and moduli values become comparable to that of the control group. Swelling was able to return mechanical properties to a pre-dried state and remove variance from the samples.

HYDRAFIL™ demonstrates an ability to resist expulsion after with as little as 1 minute in the body. However, the tests suggest that the gel may still be capable of flowing, just not through a 17-G port. Rheology testing showed gelation not being

reached until after 292±165 seconds on average, and gel was able to travel through the wax port after 9 minutes during expulsion testing.

Once in the body, HYDRAFIL™ shows capability to self-correct and match its hydration level to the environment it's in. This allows HYDRAFIL™ to self correct for any hydration loss during storage, but also helps restore biomechanics to the tissue. By maintaining proper hydration levels, nucleus pulposus replacement devices are able to restore disc height and are better suited for handling compressive loads [10].

Chapter 6

Biomechanics of Hydrogel for Nucleus Pulposus Replacement

6.1. Introduction

Success of an orthopedic implant is dependent on its ability to provide the desired biomechanics to the surrounding anatomy and capability to interface with the surrounding tissue [78]. To better predict the behavior of the hydrogel *in situ*, tests can be developed simulating the intended environment of the implant and used to evaluate performance.

Nucleus Pulposus Replacement devices have unique challenges they must face. In addition to providing stabilization to the area like other orthopedic implants, they must also facilitate hydration of the surrounding tissue and maintain disc height [57]. Throughout the day, the nucleus pulposus will lose hydration in response to force. During periods of inactivity, such as sleep, a healthy disc is able to recover water, leading to an increase in disc height. Implants must be able to integrate in the disc and resist expulsion [10].

There are several factors to a nucleus pulposus device being successful. It must be able to lose and absorb water in response to mechanical force, also leading to height changes in the disc. Hydrogels generally have low mechanical strength. In order for the implant to properly fulfill it's load bearing requirements it must show a high strength in the expected load environment (confinement) [14]. Successfully being able to handle loads should correlate to an increase in stability of the disc, which can be measured through mechanical stiffness. The integration of the gel into the tissue can be measured by the force required to extract the implant from the tissue.

6.2. Methods

HYDRAFIL™ was prepared for use through a 30 minute 121°C steam autoclave cycle using a Tuttnauer 2540 autoclave. Gel was put into the autoclave inside of injection devices provided by ReGelTec. After autoclaving, gels were held at 65°C in a hot water bath until use.

Mechanical force for expulsion was applied through the use of a Shimadzu EZ-X tensile tester. This machine was used for both compressive and tensile forces. Settings for each test were specified in their respective sections.

6.2.1. Height Recovery

Height Recovery was performed on cylindrical samples molded using a 20mm diameter by 8mm height mold. Samples were injection into the molds and then centrifuged on swinging plates to eliminate any air bubbles. Initial height and mass measurements were taken.

Samples were submerged in a 0.15 MPa osmotic swelling solution to mimic the osmotic conditions of the spine [79]. Solution was prepared using 128g of PEG 20k, 8.7g NaCl, and 1L of DI H2O. While in solution, samples were tested for 16 hours using a Shimadzu EZ-X. Compressive force was increased from 15N to 165N at a rate of 25 N/s and then back down to 15N at the same rate. There was a 10 second delay between each compressive cycle.

At the end of the 16-hour loading cycle, samples were tested for both height and weight. Samples were then left to recover in the same swelling solution without loading. At the end of the recovery period samples were again tested for height and weight.

Height and weight at each step were reported and normalized to the starting values. Height change at each step was recorded. Daily height recovery was calculated by dividing height gain during recovery period by the height loss in the previous loading cycle.

6.2.2. Confined Compression

Confined compression testing was performed using gel molding into a cylinder with a 20mm diameter and an 8mm height. Hydrogel was injected into a plastic mold with those dimensions and then centrifuged on swing plates to remove air bubbles in the sample. After allowing 48 hours for samples to set, they were tested on a Shimadzu EZ-X.

The first test was performed using a rigid confinement with interior dimensions matching the gel samples. A 20 mm diameter testing arm was used to compress gels within the confinement. This was followed by a compression test without the confinement using a 40 mm diameter testing arm.

Tests were performed with a strain rate of 100% strain/min until 35% strain or 400N.

6.2.3. Cadaver Mechanical Testing

Human cadaver spines were stripped and sectioned for stiffness testing. Lumbar section of the spine was divided into test specimens. Spines were cut laterally through the T12-L1 disc, L2-L3 disc, and L4-L5 disc, creating two test discs, L1-L2 and L3-L4, with a vertebral body on either side. Vertebrae were potted in Smooth Cast resin to allow it to be secured in a mechanical testing device.

After being potted, disc degeneration was evaluated by injecting a contrast material into the test and preforming a discography while it was loaded under compression using an Instron mechanical tester. Evaluations were conducted by Dr. Douglas Beall. Following contrast injection discs were placed onto a Shimadzu mechanical tester where it was cycled from -15N to 400N at 25N/s for 50 conditioning cycles, followed by 5 test cycles going from -15N to 150N at 25N/s.

Following the first set of mechanical tests, discs were injected using the HYDRAFIL™ system. A 17-gauge needle was advanced to the center of the disc and hydrogel was injected under fluoroscope. Discs were filled until gel was occupying all void space shown in the discography or until hydrogel advances outside the disc. Once injections were complete, discs were subjected to the same mechanical tests as the previous step.

After testing, results were analyzed to determine stiffness before and after implantation.

6.2.4. Bio-Integration

Discs from cadaver stiffness testing for evaluated for integration of the hydrogel into the tissue. All test specimens were cut laterally along one vertebral endplate, exposing the annulus fibrosus, nucleus pulposus, and HYDRAFIL™ implant. The remaining vertebral body was secured into a Shimadzu EZ-X. A pair of forceps were used to grip onto the implant in the tissue and then attached to the upper test fixtures of the Shimadzu EZ-X.

The testing machine was advanced at a constant rate, measuring force required to remove implant from the tissue. The hydrogel does not create any chemical adhesion to

the tissue. Resistance to expulsion was the result of the hydrogel becoming physically entangled in the disc tissue. Any non-zero result shows an amount of integration into the tissue.

Ultimate and breaking strengths were recorded from the test. Ultimate strength was the highest strength recorded during the test. Breaking strength was the last significant force before the implant was separated from the tissue.

6.2.5. Statistical Analysis

Results for Cadaver Mechanical Testing were evaluated using a one tailed ratio paired t test with a 95% confidence interval. When adding material to a sample, stiffness will only increase. A one tailed t test was used since results are only expected to change in one direction.

6.3. Results

6.3.1. Height Recovery

Average height decreased at each time point with decreasing variability. Height seemed to level off around 70% of the original height. The most drastic height changes were observed during day 1. Average height restoration on day 1 was about 40% which increased to 107% on day 6.

Samples showed an initial increase in weight, before eventually leveling off around the same starting weight. Gels tend to swell during the first day to 115% of the starting weight. As mechanical force was cycled onto the samples, hydration level equilibrates around the starting weight.

Figure 24

Normalized Average Height Change by Day

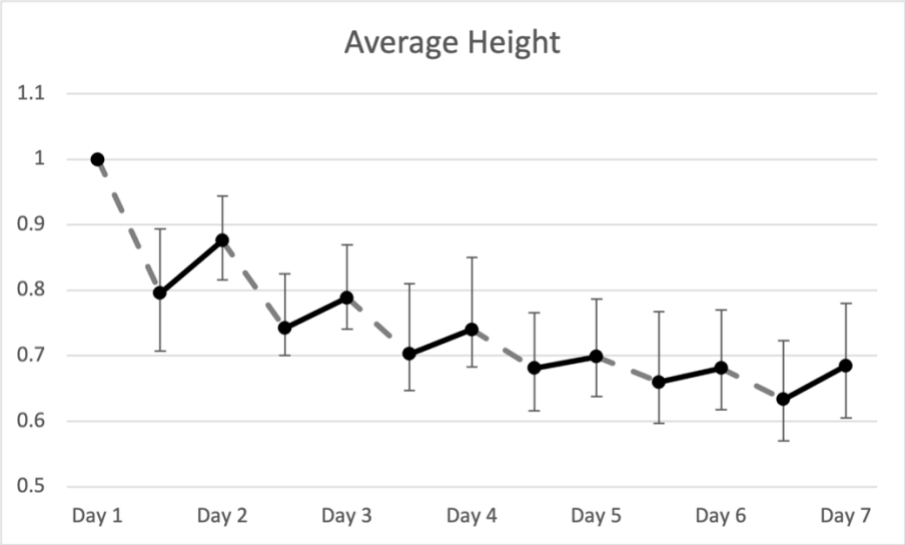

Note. Values are normalized to starting height. Error bars show maximum and minimum value obtained in any sample at each step. Dashed line represents periods of loading, solid line represents periods of unloading.

Figure 25

Average Weight Change by Day

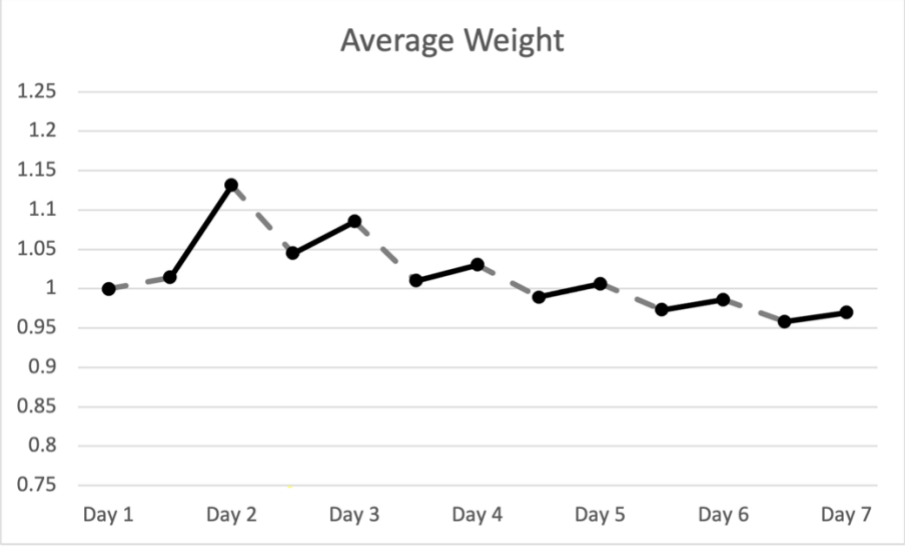

Note. Values are normalized to starting height. Dashed line represents periods of loading, solid line represents periods of unloading.

Figure 26

Daily Height Restoration

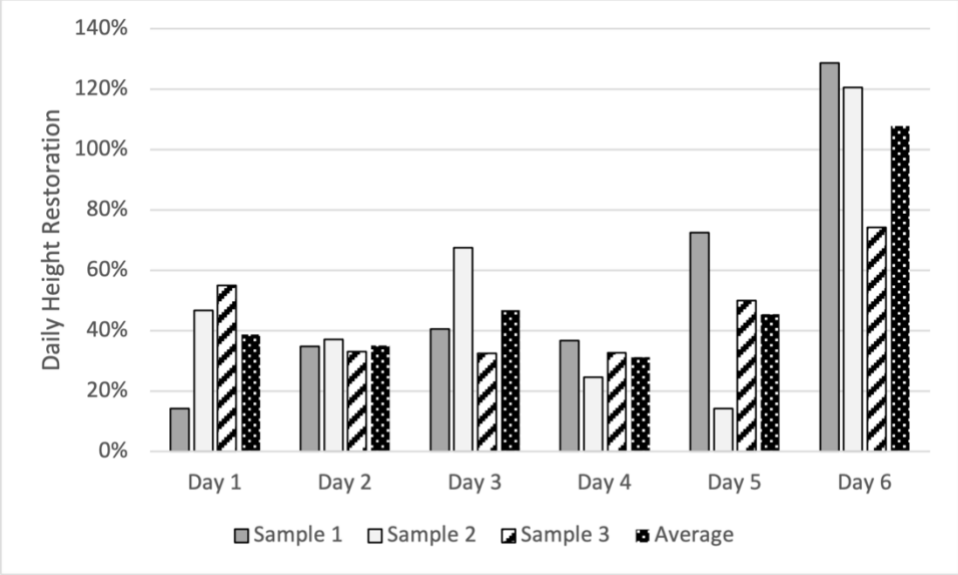

Note. Height Restoration was calculated by dividing the height gain during the unloading period by the height loss during the loading period.

6.3.2. Confined Compression

Similar to other biphasic materials, HYDRAFIL™ shows significantly ($p<0.000001$) increased moduli during confined compression testing. On average, modulus increased by 1310% (from 1.273±0.139 MPa to 16.487±0.147 MPa). Confined tests gave similar results, despite variances in the unconfined result. Results for each sample are shown in **Table *6*** below.

Graphs for confined vs unconfined mechanical testing can be seen in ***Figure 27*** and ***Figure 28*** below. Providing a confinement creates a sharp increase in mechanical strength.

Table 6

Confined vs Unconfined Compression

Sample	Modulus Confined (MPa)	Modulus Unconfined (MPa)
1	16.416	1.411
2	16.430	1.323
3	16.480	1.393
4	16.504	1.296
5	16.330	1.150
6	16.761	1.063
Average	16.487	1.273
Standard Deviation	0.147	0.139

Figure 27

Confined vs Unconfined - Sample 1

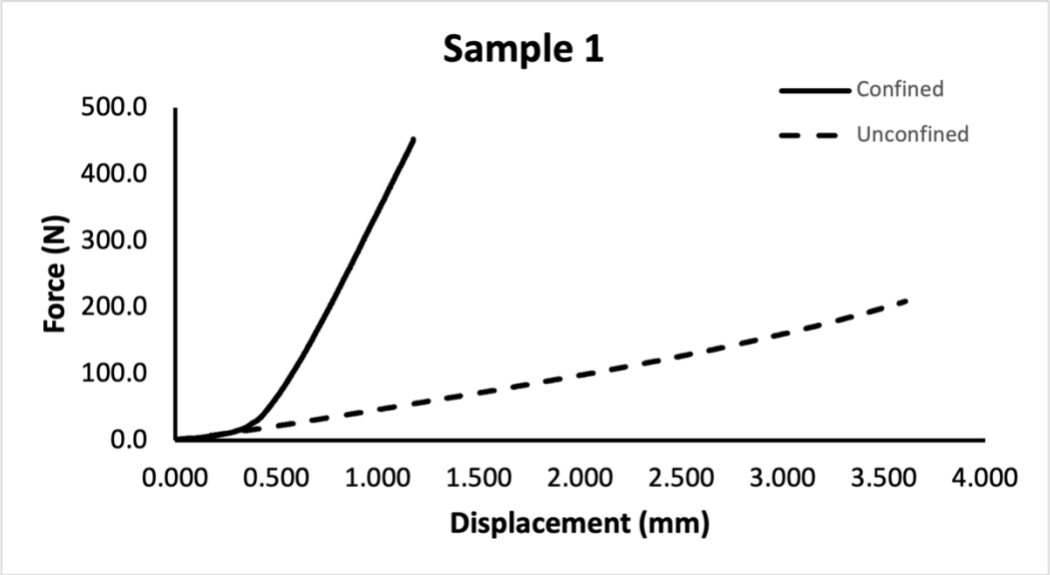

Note. Modulus values are 16.416 MPa and 1.411 MPa for Confined and Unconfined respectively

Figure 28

Confined vs Unconfined - Sample 2

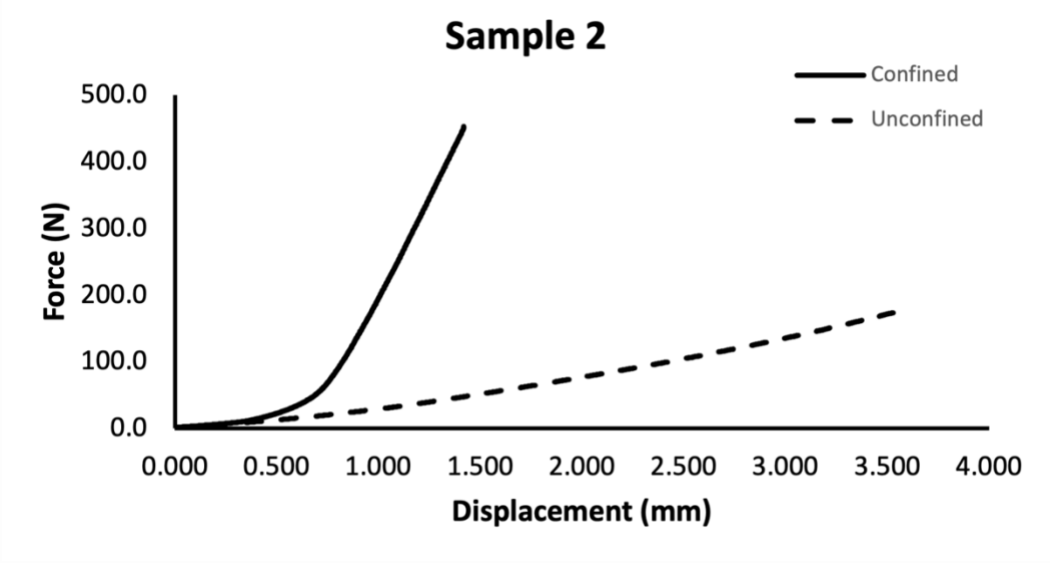

Note. Modulus values are 16.430 MPa and 1.323 MPa for Confined and Unconfined respectively

6.3.3. Cadaver Mechanical Testing

Force vs Displacement for a specific L1-L2 disc is shown below (***Figure 29***). All 6 discs tested showed an increase in stiffness post injection (See ***Table 7***). Stiffness before injection ranged from 80.5 N/mm to 294.9 N/mm. Stiffness varied greatly patient to patient and between discs of the same patient.

Post injection stiffness ranged from 96.7 N/mm to 329.8 N/mm. Stiffness significantly increased ($p<0.05$) at the test load, varying from 5% to 107%. Although some discs showed minimal change. Change in stiffness for each disc is shown in ***Figure 30*** below. There was no apparent correlation between disc/ patient and stiffness change. L1-L2 from a specific patient (1803648N) showed the greatest increase in stiffness and has the greatest overall stiffness post injection. Force vs Displacement for this disc is shown below in **Figure *29***. Discs with more drastic changes in stiffness also showed a much more linear relationship between force and displacement, showing an increased stabilization in that disc.

Table 7

Stiffness Change - Treated Human Cadaver

Disc		Displacement (mm) 150N	Displacement (mm) 400N	Stiffness (N/mm) 150N	Stiffness (N/mm) 400N	Stiffness Change 150N	Stiffness Change 400N
L1-L2 1803648N	Contrast	0.95	1.76	159.45	226.96	107%	39%
	Hydrafil	0.46	1.27	329.78	315.09		
L3-L4 1803648N	Contrast	0.58	1.41	261.18	281.75	5%	1%
	Hydrafil	0.55	1.41	273.30	283.59		
L1-L2 1809302N	Contrast	1.85	2.83	80.55	141.50	20%	5%
	Hydrafil	1.55	2.68	96.73	149.24		
L3-L4 1809302N	Contrast	1.58	1.97	96.53	203.04	98%	17%
	Hydrafil	0.79	1.68	191.61	238.39		
L1-L2 1802217M	Contrast	0.56	1.33	267.76	300.40	10%	3%
	Hydrafil	0.51	1.30	294.92	308.56		
L3-L4 1802217M	Contrast	0.50	1.53	294.98	261.65	11%	10%
	Hydrafil	0.46	1.39	326.35	287.93		

Note. Stiffness increased in each disc after HYDRAFIL™ injection. Greater changes were observed at lower loads.

Figure 29

Stiffness Change L1-L2 1803648N

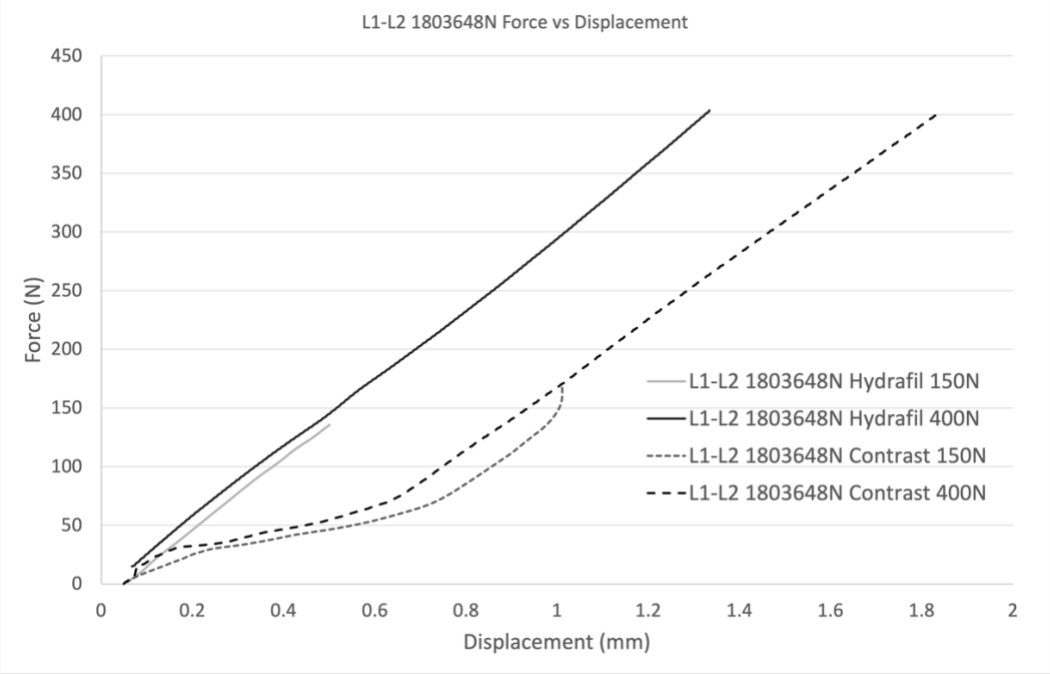

Note. Non-linear relationship of Force vs Displacement in preimplant test indicates lack of stability in disc.

Figure 30

Stiffness Difference After Injection

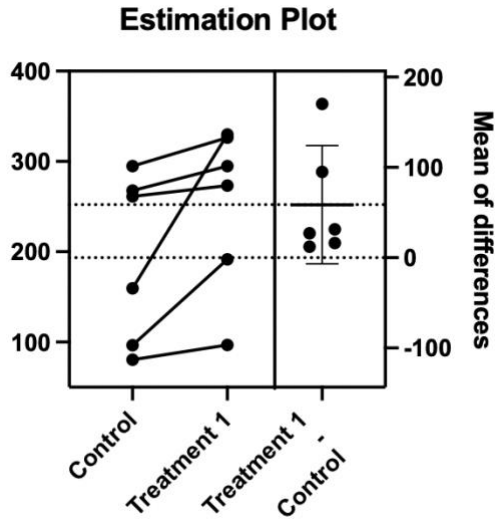

6.3.4. Bio-Integration

Bio-integration tests were performed on discs following stiffness testing. Ultimate strength during explantation ranged from 4.243N to 26.014N. Breaking strength ranged from 1.780N to 5.902N. Values for each disc are shown in **Table *8*** below. Samples with larger ultimate strengths tended to have gel expanded more laterally in the disc.

In disc L3-L4 1803648, gel formed into a horseshoe shape. While explanting, one end of the horseshoe was removed from the tissue while the other end broke from the rest of the implant. A second explantation test was performed for the other side. The two pieces had ultimate strengths of 8.361N and 13.334N and breaking strengths were 5.902N and 4.488N.

Table 8

Biointegration - Ultimate and Breaking Strengths

Disc	Ultimate Strength (N)	Breaking Strength (N)
L1-L2 1802217	8.743	5.746
L3-L4 1802217	11.852	3.533
L1-L2 1803648	4.243	1.780
L3-L4 1803648 (1)	8.361	5.902
L3-L4 1803648 (2)	13.334	4.488
L1-L2 1809302	10.640	3.226
L3-L4 1809302	26.014	3.625

Note. During explantation of disc L3-L4 1803648, roughly half of the implant broke away during the first test (1). The rest of the implant was removed during a subsequent test (2).

6.4. Discussion

HYDRAFIL™ was able to show promise as a potential nucleus pulposus replacement device. Gel samples demonstrated a strong capability to lose and gain water in response to force. When subjected to mechanical cycling during a 16-hour period samples lost both height and weight. During 8-hour periods of unloading, samples were able to regain both height and weight. For proper function of the implant, the gel should be able to regain all lost water from the 16-hour period during the 8 hours of unloading. At early timepoints the gel demonstrated unrecoverable losses in height, however total weight of the samples increased.

The most significant height losses occurred on Day 1, averaging about 20%, with only about 7.5% of the original height being recovered. Daily height recoveries varied,

but generally trended up with time (increasing from 39% to 108%). Samples demonstrated the best results on day 6, where on average the gel was able to have complete height restoration from the previous day. These were ideal results for this test, however tests should be extended to a longer time frame to confirm that the sample equilibrate at this value.

Despite the most significant height losses occurring on Day 1, it was the only day where weight increased both during the loading and unloading period. On average, weight increased by 1.4% during the first loading period and then an additional 12% during the first unloading period. Overall, weight increased by 13% on Day 1 while there was a 14% height loss after the unloading period. Weight stabilized around Day 5, where the weight was about 100% of the starting.

Significant height changes during early time points were likely due to deformation of the polymer, rather than fluid exchange. After autoclaving for the molding process, the hydrogel has a low mechanical strength due to a lack of crystallinity. As crystallinity builds the gel becomes stiffer, increasing the polymer's ability to resist deformation [17]. Increasing weight during early time points cause the material to expand outward while losing height.

Preventing outward expansion also increases the gel's mechanical strength. A hydrogel can provide strength to a structure if it is in a confinement. Biphasic material specifically has significantly increased strength inside of confinements. This is due to the liquid phased becoming trapped and acting as an incompressible once the polymer has compressed as much as it can.

Confinement would likely reduce height loss experienced during Day 1 testing. It is also possible that there are improved results in vivo since the annulus fibrosus would be able to act as a soft confinement for the hydrogel, further increasing its ability to increase mechanical strength.

In cadaveric human lumbar discs, HYDRAFIL™ was able to increase stiffness up to 107%. Stiffness changes varied greatly disc to disc, even within the same patient. All discs had a positive increase in stiffness post implant, with the smallest increase being 5%. The effectiveness of a nucleus pulposus replacement can vary greatly depending on the condition of the spinal disc. Discs with low stiffness changes showed a more linear relationship between force and displacement during pre-implant testing. Discs lacking stabilization before implantation had the largest change. Stiffness changes were greater at lower compressive forces.

A secondary endpoint of stiffness testing was to ensure that the implant stayed in place when loaded. Migration is a large concern for any nucleus pulposus replacement device. Not only if the device not able to properly function if outside the intended space, but close proximity to the spinal creates larger concerns of possible neural damage [10]. No expulsions were observed during testing and hydrogel stay in place within the disc. To ensure that HYDRAFIL™ has interfaced with the surrounding tissue, the biointegration can be tested. Biointegration in this case was a measurement of how much force it takes to remove the implant from the tissue. Discs were cut along one endplate, exposing the annulus and nucleus. Hydrogel was then latched onto with forceps attached to a tensile testing device.

Maximum force recorded during explantation was 26N. Implants were well integrated with the annulus and took a relatively high amount of force to remove. In one case, the implant broke into two pieces before separating from the tissue. Samples with higher values tended to expand more radially into the annulus. HYDRAFIL™ was observed to fill into transdiscal tears and in between some lamella. This demonstrates a resistance to expulsion and an integration with the native tissue.

Results showed potential for HYDRAFIL™ to be used as a nucleus pulposus replacement device. It has demonstrated a capability to restore disc height and resist mechanical force. HYDRAFIL™ has considerable increased strength when used within a confinement. Possibly most important, once set HYDRAFIL™ resists expulsion and does not migrate within the disc.

Chapter 7

Conclusions and Future Work

HYDRAFIL™ has shown promise as a minimally invasive nucleus pulposus replacement device that can be used to bridge the current gap in coverage for degenerative disc disease. HYDRAFIL™ has demonstrate reversibility for both gelation and crystallization using a 121°C autoclave cycle. Reversing both of these properties were essential for ensure flow, and therefore injection of the gel. Crystallinity was shown to significantly increase over time in both storage and physiological conditions, however even the increased levels were reversed with the proposed autoclave cycle of 121°C for 30 mins.

HYDRAFIL™ was shown to stay in a flowable state when held at 65°C and had an undefined gelation at 62°C. This is likely the temperature that gelation occurs and can be considered the gel temperature of the hydrogel, similar to a melting temperature. Even after 24 hours, HYDRAFIL™ was still flowable at the 65°C set point. HYDRAFIL™ should be held above this temperature prior to injection to ensure flow.

HYDRAFIL™ was capable of curing *in situ* over the course of a few minutes. On average gelation occurred after 292±165 seconds, but demonstrated a resistance to expulsion at times as short as 1 minute. Despite rheological testing showing the gel to still be flowable after 1 minute, it has stiffened enough that the shear forces experienced by the gel were too great to force it through the expulsion port at those mechanical loads.

The gel also demonstrated an ability to recover potential lost hydration during storage. Gels were partially dried before testing for modulus then retested after 1 week in body conditions (held at 37°C and submerged in a 0.15M swelling solution) to examine

their ability to recover lost hydration. Gels with mild dehydration (having lost about 25% or their original water content) did not show a significant difference in strength either pre- or post-swelling, but dryer samples (having lost about 65% of their original water content) demonstrated a significantly higher modulus in pre-swelling tests. In post swelling tests there were no was no significant difference in moduli values between any groups. Follow up studies increasing the number of samples in these tests might provide a greater confidence level and show a significant difference between the control and mild dehydration groups.

Once set in the body, the gel demonstrates an ability to restore biomechanics of the tissue. When placed under cyclic loads designed to mimic daily activity in a spine the gel lost water in repose to force. During periods of unloading, the gel was able to restore hydration as well as height. Effects were most prevalent on final day of testing. Future work should extend these studies to further timepoints to confirm these effects are lasting.

Despite being relatively weak on its own, HYDRAFIL™ demonstrated significantly higher strengths under confinement. This shows promise in its ability to perform as a nucleus pulposus replacement device where it will be under a soft confinement of the annulus fibrosus. When injected into cadaver tissue, implantation had varying results on stiffness change. Some samples showed very drastic increases while others had almost no change. This is likely due to high variation of degeneration between samples, even within the same patient and unrepeatable injection procedures. Discs do not degenerate in a controlled manor, HYDRAFIL™ fills in each disc differently depending on how the tissue was damaged. Furthermore, more compromised annuli are going to be less capable

of containing substantial amounts of hydrogel. Despite this, HYDRAFIL™ still showed a significant increase in stiffness after implantation ($p<0.05$).

Once implanted, HYDRAFIL™ demonstrated an ability to integrate with the tissue. During cyclic mechanic testing of cadaver samples, there was no noticeable migration of the gel in the disc. Migration of nucleus pulposus replacement devices is a large concern due to their proximity to the spinal cord. Tests were developed to determine amount of force required to remove the implant from the disc showed forces as high as 26N. Gel with a higher resistance to explantation tended to spread circumferentially through the annulus. Resistance appeared to be from physical entrapment of the gel within the fibers of the tissue, opposed to chemical adhesion. All samples demonstrated a resistance to expulsion and migration. Future work should be developed to investigate to migration and expulsion of HYDRAFIL™ had different injection pressures. Higher pressures may lead to a larger interface between the tissue and implant but may also make the gel more prone to migration. This relationship should be understood to ensure safe delivery to patients.

HYDRAFIL™ successfully demonstrated an ability to act as a nucleus pulposus replacement device. It is capable of being held in a flowable state for safe injection. It sure *in situ* over a relatively short amount of time and resists expulsion. Once in the body, it integrates well with the tissue, increases mechanical strength, and restores biomechanics.

References

[1] A. Wu *et al.*, "Global low back pain prevalence and years lived with disability from 1990 to 2017: estimates from the Global Burden of Disease Study 2017," *Ann. Transl. Med.*, vol. 8, no. 6, pp. 299–299, 2020.

[2] F. Fatoye, T. Gebrye, and I. Odeyemi, "Real-world incidence and prevalence of low back pain using routinely collected data," *Rheumatol. Int.*, vol. 39, no. 4, pp. 619–626, 2019.

[3] B. McHugh, "What Is Degenerative Disc Disease?," *Spine Health*, 2017. [Online]. Available: https://www.spine-health.com/conditions/degenerative-disc-disease/what-degenerative-disc-disease.

[4] "Artificial discs for lumbar and cervical degenerative disc disease -update: an evidence-based analysis.," *Ont. Health Technol. Assess. Ser.*, vol. 6, no. 10, pp. 1–98, 2006.

[5] J. Fernandez-Moure *et al.*, "Novel therapeutic strategies for degenerative disc disease: Review of cell biology and intervertebral disc cell therapy," *SAGE Open Med.*, vol. 6, p. 205031211876167, 2018.

[6] "Study supports use of VIA Disc to treat degenerative disc disease," *Spinal News International*, 2020. .

[7] T. M. Irmola, A. Häkkinen, S. Järvenpää, I. Marttinen, K. Vihtonen, and M. Neva, "Reoperation Rates Following Instrumented Lumbar Spine Fusion," *Spine (Phila. Pa. 1976).*, vol. 43, no. 4, 2018.

[8] M. Bydon, R. De la Garza-Ramos, M. Macki, A. Baker, A. K. Gokaslan, and A. Bydon, "Lumbar fusion versus nonoperative management for treatment of discogenic low back pain: a systematic review and meta-analysis of randomized controlled trials.," *J. Spinal Disord. Tech.*, vol. 27, no. 5, pp. 297–304, Jul. 2014.

[9] A. Carl, E. Ledet, H. Yuan, and A. Sharan, "New developments in nucleus pulposus replacement technology," *Spine J.*, vol. 4, no. 6 SUPPL., pp. S325–S329, 2004.

[10] M. L. Goins, D. W. Wimberley, P. S. Yuan, L. N. Fitzhenry, and A. R. Vaccaro, "Nucleus pulposus replacement: An emerging technology," *Spine J.*, vol. 5, no. 6 SUPPL., pp. S317–S324, 2005.

[11] G. Tendulkar, T. Chen, S. Ehnert, H. P. Kaps, and A. K. Nüssler, "Intervertebral disc nucleus repair: Hype or hope?," *Int. J. Mol. Sci.*, vol. 20, no. 15, 2019.

[12] M. L. Goins, D. W. Wimberley, P. S. Yuan, L. N. Fitzhenry, and A. R. Vaccaro, "Nucleus pulposus replacement: an emerging technology.," *Spine J.*, vol. 5, no. 6 Suppl, pp. 317S-324S, 2005.

[13] T. Lee, T.-H. Lim, S.-H. Lee, J.-H. Kim, and J. Hong, "Biomechanical function of a balloon nucleus pulposus replacement system: A human cadaveric spine study," *J. Orthop. Res.*, vol. 36, no. 1, pp. 167–173, 2018.

[14] A. Joshi *et al.*, "Functional compressive mechanics of a PVA/PVP nucleus pulposus replacement," *Biomaterials*, vol. 27, no. 2, pp. 176–184, 2006.

[15] "ReGelTec." [Online]. Available: https://regeltec.com.

[16] J. H. Lee, "Injectable hydrogels delivering therapeutic agents for disease treatment and tissue engineering," *Biomater. Res.*, vol. 22, pp. 1–14, 2018.

[17] V. Lamastro, E. Brewer, and A. Lowman, "Crystallinity, reversibility, and injectability of physically crosslinked poly(vinyl alcohol) and poly(ethylene glycol) hydrogels," *J. Appl. Polym. Sci.*, vol. 31 October, 2019.

[18] G. Kayalioglu, "Chapter 3 - The Vertebral Column and Spinal Meninges," in *The Spinal Cord*, C. Watson, G. Paxinos, and G. Kayalioglu, Eds. San Diego: Academic Press, 2009, pp. 17–36.

[19] A. R. Burdi, D. F. Huelke, R. G. Snyder, and G. H. Lowrey, "Infants and children in the adult world of automobile safety design: Pediatric and anatomical considerations for design of child restraints," *J. Biomech.*, vol. 2, no. 3, pp. 267–280, 1969.

[20] A. M. Christensen, N. V Passalacqua, and E. J. Bartelink, "Chapter 4 - Medicolegal Significance," in *Forensic Anthropology*, A. M. Christensen, N. V Passalacqua, and E. J. Bartelink, Eds. San Diego: Academic Press, 2014, pp. 91–117.

[21] P. J. Mansfield and D. A. Neumann, "Chapter 8 - Structure and Function of the Vertebral Column," in *Essentials of Kinesiology for the Physical Therapist Assistant (Third Edition)*, Third Edit., P. J. Mansfield and D. A. Neumann, Eds. St. Louis (MO): Mosby, 2019, pp. 178–232.

[22] G. Gillen, "Chapter 18 - Trunk Control: Supporting Functional Independence," in *Stroke Rehabilitation (Fourth Edition)*, Fourth Edi., G. Gillen, Ed. Mosby, 2016, pp. 360–393.

[23] S. J. Hall, *Basic Biomechanics*, 5th ed. New York, NY: McGraw-Hill, 2007.

[24] A. Rossdeutsch, P. Copley, and S. Khan, “Degenerative spinal disc disease and its treatment,” *Orthop. Trauma*, vol. 31, no. 6, pp. 378–387, Dec. 2017.

[25] R. J. Moore, “The vertebral endplate: disc degeneration, disc regeneration.,” *Eur. spine J. Off. Publ. Eur. Spine Soc. Eur. Spinal Deform. Soc. Eur. Sect. Cerv. Spine Res. Soc.*, vol. 15 Suppl 3, no. Suppl 3, pp. S333-7, Aug. 2006.

[26] F. Del Grande, T. P. Maus, and J. A. Carrino, “Imaging the intervertebral disk: age-related changes, herniations, and radicular pain.,” *Radiol. Clin. North Am.*, vol. 50, no. 4, pp. 629–649, Jul. 2012.

[27] F. Galbusera and M. Van Rijsbergen, “Ageing and degenerative changes of the intervertebral disc and their impact on spinal flexibility,” vol. 23, pp. 324–332, 2014.

[28] J. C. Lotz, A. J. Fields, and E. C. Liebenberg, “The role of the vertebral end plate in low back pain.,” *Glob. spine J.*, vol. 3, no. 3, pp. 153–164, Jun. 2013.

[29] F. Travascio, M. Eltoukhy, and S. Asfour, “Spine Biomechanics: A Review of Current Approaches,” 2015.

[30] R. Izzo, G. Guarnieri, G. Guglielmi, and M. Muto, “Biomechanics of the spine. Part I: Spinal stability,” *Eur. J. Radiol.*, vol. 82, no. 1, pp. 118–126, 2013.

[31] K. J. Lorme, “THE BIOMECHANICS OF BACK PAIN.,” *Australasian Chiropractic & Osteopathy*, vol. 11, no. 1. p. 37, Mar-2003.

[32] F. Galbusera, *Biomechanics of the Spine : Basic Concepts, Spinal Disorders and Treatments*. San Diego, UNITED KINGDOM: Elsevier Science & Technology, 2018.

[33] T. R. Oxland, “A history of spine biomechanics,” *Unfallchirurg*, vol. 118, no. 1, pp. 80–92, 2015.

[34] K. B. Broberg, “On the mechanical behaviour of intervertebral discs.,” *Spine (Phila. Pa. 1976).*, vol. 8, no. 2, pp. 151–165, Mar. 1983.

[35] J. S. Shah, W. G. Hampson, and M. I. Jayson, “The distribution of surface strain in the cadaveric lumbar spine.,” *J. Bone Joint Surg. Br.*, vol. 60-B, no. 2, pp. 246–251, May 1978.

[36] M. Kolber and W. Hanney, “The dynamic disc model: a systematic review of the literature,” *Phys. Ther. Rev.*, vol. 14, pp. 181–189, 2009.

[37] B. Vernon-Roberts, R. J. Moore, and R. D. Fraser, "The natural history of age-related disc degeneration: The pathology and sequelae of tears," *Spine (Phila. Pa. 1976).*, vol. 32, no. 25, pp. 2797–2804, 2007.

[38] M. A. Adams and P. Dolan, "Intervertebral disc degeneration: Evidence for two distinct phenotypes," *Journal of Anatomy*, vol. 221, no. 6. pp. 497–506, 2012.

[39] A. Beierfuß *et al.*, "Knockout of Apolipoprotein E in rabbit promotes premature intervertebral disc degeneration : A new in vivo model for therapeutic approaches of spinal disc disorders," pp. 1–18, 2017.

[40] Y. Zhang, H. S. An, C. Tannoury, E. J. M. A. Thonar, M. K. Freedman, and D. G. Anderson, "Biological treatment for degenerative disc disease: Implications for the field of physical medicine and rehabilitation," *Am. J. Phys. Med. Rehabil.*, vol. 87, no. 9, pp. 694–702, 2008.

[41] J. M. Highsmith, "Physical Therapy for Degenerative Disc Disease," *Spine Universe*, 2019. [Online]. Available: https://www.spineuniverse.com/conditions/degenerative-disc/physical-therapy-degenerative-disc-disease.

[42] W. Shi, E. Agbese, A. Z. Solaiman, D. L. Leslie, and D. R. Gater, "Performance of Pain Interventionalists From Different Specialties in Treating Degenerative Disk Disease-Related Low Back Pain," *Arch. Rehabil. Res. Clin. Transl.*, vol. 2, no. 3, p. 100060, 2020.

[43] E. Rasmussen-Barr, L. Nilsson-Wikmar, and I. Arvidsson, "Stabilizing training compared with manual treatment in sub-acute and chronic low-back pain," *Man. Ther.*, vol. 8, no. 4, pp. 233–241, 2003.

[44] D. K. Park, "Spinal Fusion," *OrthoInfo*, 2018. [Online]. Available: https://orthoinfo.aaos.org/en/treatment/spinal-fusion/.

[45] R. J. Mobbs, K. Phan, G. Malham, K. Seex, and P. J. Rao, "Lumbar interbody fusion: techniques, indications and comparison of interbody fusion options including PLIF, TLIF, MI-TLIF, OLIF/ATP, LLIF and ALIF.," *J. spine Surg. (Hong Kong)*, vol. 1, no. 1, pp. 2–18, 2015.

[46] K. S. Dhillon, "Spinal fusion for chronic low back pain: A 'Magic Bullet' or wishful thinking?," *Malaysian Orthop. J.*, vol. 10, no. 1, pp. 61–68, 2016.

[47] J. I. Brox, Ø. P. Nygaard, I. Holm, A. Keller, T. Ingebrigtsen, and O. Reikerås, "Four-year follow-up of surgical versus non-surgical therapy for chronic low back pain," *Ann. Rheum. Dis.*, vol. 69, no. 9, pp. 1643–1648, 2010.

[48] I. A. Harris, A. Traeger, R. Stanford, C. G. Maher, and R. Buchbinder, “Lumbar spine fusion: what is the evidence?,” *Intern. Med. J.*, vol. 48, no. 12, pp. 1430–1434, 2018.

[49] “Lumbar Disk Replacement,” *Johns Hopkins Medicine*. [Online]. Available: https://www.hopkinsmedicine.org/health/treatment-tests-and-therapies/lumbar-disk-replacement.

[50] J. Spivak, “Artificial Disc Replacement or Spinal Fusion: Which is Better for You?,” *Spine Health*, 2006. [Online]. Available: https://www.spine-health.com/treatment/back-surgery/artificial-disc-replacement-or-spinal-fusion-which-better-you.

[51] K. D. van den Eerenbeemt, R. W. Ostelo, B. J. van Royen, W. C. Peul, and M. W. van Tulder, “Total disc replacement surgery for symptomatic degenerative lumbar disc disease: a systematic review of the literature.,” *Eur. spine J. Off. Publ. Eur. Spine Soc. Eur. Spinal Deform. Soc. Eur. Sect. Cerv. Spine Res. Soc.*, vol. 19, no. 8, pp. 1262–1280, Aug. 2010.

[52] S. Cai, Y. Tian, J. Zhang, J. Hu, and F. Chen, “Efficacy and Safety of Total Disc Replacement compared with Anterior Cervical Discectomy and Fusion in the Treatment of Cervical Disease: A Meta-analysis,” *Spine (Phila. Pa. 1976).*, vol. 45, no. 20, 2020.

[53] X. D. Cui, H. T. Li, W. Zhang, L. L. Zhang, Z. P. Luo, and H. L. Yang, “Mid- to long-term results of total disc replacement for lumbar degenerative disc disease: A systematic review,” *J. Orthop. Surg. Res.*, vol. 13, no. 1, pp. 1–12, 2018.

[54] K. Della Volpe and S. Spinasanta, “Cervical Artificial Disc Replacement Outcomes at 5 to 10 Years,” *Spine Universe*, 2019. .

[55] A. Di Martino, A. R. Vaccaro, J. Y. Lee, V. Denaro, and M. R. Lim, “Nucleus pulposus replacement: basic science and indications for clinical use.,” *Spine (Phila. Pa. 1976).*, vol. 30, no. 16 Suppl, pp. S16-22, Aug. 2005.

[56] J. R. Meakin, J. E. Reid, and D. W. L. Hukins, “Replacing the nucleus pulposus of the intervertebral disc,” *Clin. Biomech.*, vol. 16, no. 7, pp. 560–565, 2001.

[57] G. Lewis, “Nucleus pulposus replacement and regeneration/repair technologies: Present status and future prospects,” *J. Biomed. Mater. Res. B. Appl. Biomater.*, vol. 100, pp. 1702–1720, Aug. 2012.

[58] L. Zengerle, A. Köhler, E. Debout, C. Hackenbroch, and H. J. Wilke, “Nucleus replacement could get a new chance with annulus closure,” *Eur. Spine J.*, vol. 29, no. 7, pp. 1733–1741, 2020.

[59] E. Caló and V. V. Khutoryanskiy, “Biomedical applications of hydrogels: A review of patents and commercial products,” *Eur. Polym. J.*, vol. 65, pp. 252–267, 2015.

[60] A. S. Hoffman, “Hydrogels for biomedical applications,” *Adv. Drug Deliv. Rev.*, vol. 64, no. SUPPL., pp. 18–23, 2012.

[61] S. H. Aswathy, U. Narendrakumar, and I. Manjubala, “Commercial hydrogels for biomedical applications,” *Heliyon*, vol. 6, no. 4, p. e03719, 2020.

[62] Q. Chai, Y. Jiao, and X. Yu, “Hydrogels for Biomedical Applications: Their Characteristics and the Mechanisms behind Them,” *Gels*, vol. 3, no. 1, 2017.

[63] W. Nafo and A. Al-Mayah, “Mechanical characterization of PVA hydrogels’ rate-dependent response using multi-axial loading,” *PLoS One*, vol. 15, no. 5, pp. 1–16, 2020.

[64] A. Kumar and S. S. Han, “PVA-based hydrogels for tissue engineering: A review,” *Int. J. Polym. Mater. Polym. Biomater.*, vol. 66, no. 4, pp. 159–182, 2017.

[65] D. A. Subramanian, “The Use of Poly (vinyl alcohol) -based Hydrogels in Biomedical Applications,” pp. 1–58, 2018.

[66] Z. Xu *et al.*, “Morphological and swelling behavior of cellulose nanofiber (CNF)/poly(vinyl alcohol) (PVA) hydrogels: poly(ethylene glycol) (PEG) as porogen,” *RSC Adv.*, vol. 6, no. 49, pp. 43626–43633, 2016.

[67] N. P. Money, “Osmotic Pressure of Aqueous Polyethylene Glycols,” *Plant Physiol.*, vol. 91, no. 2, pp. 766–769, 1989.

[68] V. R. Binetti, G. W. Fussell, and A. M. Lowman, “Evaluation of two chemical crosslinking methods of poly(vinyl alcohol) hydrogels for injectable nucleus pulposus replacement,” *J. Appl. Polym. Sci.*, vol. 131, no. 19, pp. 1–8, 2014.

[69] G. Tegze *et al.*, “Diffusion-controlled anisotropic growth of stable and metastable crystal polymorphs in the phase-field crystal model,” *Phys. Rev. Lett.*, vol. 103, no. 3, pp. 1–4, 2009.

[70] J. L. Holloway, A. M. Lowman, and G. R. Palmese, “The role of crystallization and phase separation in the formation of physically cross-linked PVA hydrogels,” *Soft Matter*, vol. 9, no. 3, pp. 826–833, 2013.

[71] L. C. Tsen and D. L. Hepner, “Needles used for spinal anesthesia,” *Expert Rev. Med. Devices*, vol. 3, no. 4, pp. 499–508, 2006.

[72] "ReGelTec Receives FDA Breakthrough Designation for its HYDRAFIL™ System," *Business Wire*, 2020. [Online]. Available: https://www.businesswire.com/news/home/20201209005150/en/ReGelTec-Receives-FDA-Breakthrough-Designation-for-its-HYDRAFIL™-System.

[73] R. L. Blaine, "Determination of Polyethylene Crystallinity by DSC," *TA Instruments*, vol. 2002, no. 09, pp. 1–3, 2002.

[74] ASTM International, "F2346-18 - Standard Test Methods for Static and Dynamic Characterization of Spinal Artificial," West Conshohocken, PA, 2014.

[75] by Priyanka Preyas Shah, "Optimization of the Endplate Interface for a Surrogate Intervertebral Disc Model for Wear and Fatigue Testing of Nucleus Pulposus Replacement Devices," 2009.

[76] S. E. Bezci and G. D. O'Connell, "Osmotic Pressure Alters Time-dependent Recovery Behavior of the Intervertebral Disc," *Spine (Phila. Pa. 1976).*, vol. 43, no. 6, pp. E334–E340, 2018.

[77] ASTM International, "F2789-10 - Standard Guide for Mechanical and Functional Characterization of Nucleus," West Conshohocken, PA, 2010.

[78] X. Gao, M. Fraulob, and G. Haïat, "Biomechanical behaviours of the bone-implant interface: A review," *J. R. Soc. Interface*, vol. 16, no. 156, 2019.

[79] J. P. G. Urban and J. F. McMullin, "Swelling pressure of the lumbar intervertebral discs: influence of age, spinal level, composition, and degeneration.," *Spine (Phila. Pa. 1976).*, vol. 13, no. 2, pp. 179–187, Feb. 1988.